



Strålsäkerhets
myndigheten

Swedish Radiation Safety Authority

Authors: Tero Manngård
Ali Massih
Jan-Olof Stengård

Research

2014:18

Evaluation of the Halden IFA-650
loss-of-coolant accident
experiments 2, 3 and 4

SSM perspective

Background

Loss of Coolant Accidents (LOCA) are among the most demanding accidents that can happen in a Light Water Reactor (LWR). The lack of cooling and the drop in pressure impose large stresses on the nuclear fuel which would increase the risk of fuel rod damage and the subsequent release of active material. But LOCA is also an accident that the nuclear power plant is designed to withstand with a limited release of radioactivity to the surroundings. Limitations shall be put upon the use of the nuclear fuel, that the reactor core constitutes of, such that the core can go through a LOCA without giving rise to an accelerating amount of damage, spread of active material within the power plant and its personnel nor spread of radioactivity to the environment.

Recent research has shown that nuclear fuel that has been irradiated to a high burnup can fail at lower temperatures than as prescribed by current design criteria. Ballooning and rupture of the cladding tube can occur at temperatures around 800 °C instead of the stipulated 1200 °C and the damage can result in a movement of the fissile material inside the cladding tube and release through the rupture.

The research is performed as tests in research reactors and institutes around the world, the Halden research reactor is one example. The tests need to be analyzed in order to understand the phenomena acting on the materials; i.e. how the cladding expands, in what way the fissile fuel pellets crack and move, and what makes the cladding to finally break. This understanding will hopefully make it possible to use the fuel to a higher burnup in a safe way.

Objectives

The objective for SSM in this project is to interpret the test and to implement the observed behavior of the nuclear fuel in analytical tools.

Results

The analytical tools, which are fuel rod computer codes, that Quantum Technologies AB use and develop, contain models of several of the phenomena that are acting on the nuclear fuel (cladding temperature, fission gas driven pressure, strain and stress in the cladding, rod rupture, etc.) and how the separate effects interact in the complex integrated manner. The codes are under constant development and need to be compared with actual tests. In this report simulations of three tests in Halden (IFA-650.2,3 and 4) are described.

Although it is difficult to model complex accident scenarios, the results obtained by Quantum Technologies AB show that it can be achieved. The codes and models can reasonably calculate cladding temperature, strain and diameter increase as a function of time, and finally estimate the position of cladding rupture.

Need for further research

In the future, more tests on nuclear fuel in LOCA conditions will be performed and to some extent code development will determine which aspects need to be further tested. The tests will form a base for the codes and model development around the world. When sufficiently many tests have been performed it will be possible to develop codes that with high confidence predict the behavior of the materials in the reactor core during a LOCA.

Project information

Contact person SSM: Jan In de Betou

Reference: SSM2012/510



Strål
säkerhets
myndigheten

Swedish Radiation Safety Authority

Authors: Tero Manngård¹⁾, Ali Massih¹⁾, Jan-Olof Stengård²⁾

¹⁾Quantum Technologies AB, Uppsala, Sweden

²⁾VTT Technical Research Centre of Finland

2014:18

Evaluation of the Halden IFA-650
loss-of-coolant accident
experiments 2, 3 and 4

This report concerns a study which has been conducted for the Swedish Radiation Safety Authority, SSM. The conclusions and viewpoints presented in the report are those of the author/authors and do not necessarily coincide with those of the SSM.

Contents

Abstract	III
Sammanfattning	IV
1 Introduction	1
2 Halden IFA-650 experiments	2
2.1 IFA-650.2	3
2.2 IFA-650.3	4
2.3 IFA-650.4	6
3 Computer codes	11
4 Calculations	13
4.1 Fuel rod initial state	13
4.2 Coolant conditions and plenum temperature	14
4.3 Rod gas pressure	19
4.3.1 IFA-650.2	19
4.3.2 IFA-650.3	19
4.3.3 IFA-650.4	19
4.4 Cladding deformation and rupture	22
4.4.1 IFA-650.2	22
4.4.2 IFA-650.3	22
4.4.3 IFA-650.4	23
5 Concluding remarks	27
References	30
Appendix A Input parameters for cladding models	31

Abstract

The Halden reactor fuel rod loss-of-coolant accident (LOCA) tests, IFA-650 series 2, 3, and 4, are evaluated using two versions of the computer code FRAPTRAN-1 . 4. The test sample IFA-650.2 was a fresh fuel rod, that is unirradiated, with pressurized water reactor (PWR) rod characteristics, while IFA-650.3 and IFA-650.4 sample rods were refabricated from fuel rods irradiated in a PWR to rod burnups of 82 and 92 MWd/kgU, respectively. All the rods failed during the LOCA tests at temperatures around and below 800°C by fuel cladding burst. The results of our computer calculations are compared with measured data for the following parameters: (i) Cladding temperature as a function of time; (ii) Cladding diameter at rupture versus axial position of the rod; (iii) Fuel rod pressure as a function of time; (iv) Peak cladding temperature at rupture; and (v) Maximum cladding oxide layer thickness after LOCA transient (test 2). The agreement between calculations and measurements and between the two versions of the utilized code are satisfactory. The report offers descriptions of the tests, the computer codes, the computations and a summary of the results.

Sammanfattning

Bränslestavprover under LOCA förhållanden i Halden reaktorn, IFA-650 seriens prov 2, 3, och 4, utvärderas med två olika versioner av datorprogrammet FRAPTRAN-1 . 4. Provobjektet vid IFA-650.2 var en färsk bränslestav, dvs. i obestrålat tillstånd, med stavegenskaper karakteristiska för tryckvattenreaktor (PWR) bränsle. Experimentstavarna för proven IFA-650.3 och IFA-650.4 tillverkades från bränslestavar, förbestrålade i en PWR, till en stavutbränning av 82 MWd/kgU för det första provet och 92 MWd/kgU för det andra. Alla tre bränslestavar havererade under LOCA proven vid temperaturer omkring eller under 800°C, genom kapslingsbrott. Resultaten från våra datorberäkningar jämförs med mätdata för följande parametrar: (i) kapslingstemperatur som funktion av tid; (ii) bränslestavtryck som funktion av tid; (iii) kapslingsdiameter vid brott längs staven; (iv) maximal kapslingstemperatur vid brott; och (v) maximal oxidtjocklek efter LOCA transienten (prov 2). Överensstämmelsen mellan beräkningar och mätningar samt mellan de två olika versionerna av beräkningsprogrammet är tillfredsställande. I rapporten ges beskrivningar av de olika proven, datorprogrammen, beräkningarna och en sammanfattning av resultaten.

1 Introduction

Loss of coolant accidents are postulated reactor accidents that are caused by the loss of reactor coolant at a rate in excess of the capability of the reactor coolant makeup system from breaks in the reactor coolant pressure boundary, including a break equivalent in size to the double-ended rupture of the largest pipe of the reactor coolant system (USNRC 2011). As a result of LOCA fuel cladding temperature rises well beyond the normal operating condition (≈ 580 K) while the coolant pressure can drop below the fuel rod internal pressure, leading to cladding expansion and eventual failure. There are two principal mechanisms for cladding failure, namely, excessive oxidation of zirconium alloy cladding tube and excessive outward deformation (ballooning) due to creep mechanism. The two mechanisms act in parallel until cladding tube bursts. Fuel cladding is considered as the first line of defense that provides a barrier to the release of fission products to the surrounding environment. A recent review of the literature on cladding failure under reactor accidents including LOCA can be found in (Alam, Khan, Pathak, Ravi, Singh, and Gupta 2011).

The appraisal of the consequences of LOCA, regarding the fuel system, is to a great extent based on computations performed with computer codes simulating the involved phenomena. To validate these computer codes, and the models used therein, appropriate integral fuel rod tests under LOCA conditions are needed. The IFA-650 test series, performed within the OECD Halden Reactor Project at Halden, Norway, are especially designed for this purpose. The IFA-650 series comprise both fresh fuel rods (tests 1 and 2) and high burnup rods which were irradiated in commercial pressurized water reactors or PWRs (tests 3 and 4). The conditions for the tests were planned to satisfy the following objectives (Ek 2005a): (i) to maximize the ballooning of the cladding to enhance fuel pellet relocation and examine its consequence on cladding temperature and oxidation; (ii) to investigate the extent of “secondary transient hydriding” on the cladding inner side around the burst region. Fuel relocation occurs due to an opening of, or an increase in pellet-cladding gap and possible quivering of the fuel rod due to burst. Secondary transient hydriding refers to zirconium-steam reaction at the inner side of the cladding, upon cladding burst, which releases hydrogen gas, a portion of which is absorbed by the cladding, building zirconium hydride with brittling effect.

Here, we have used the FRAPTRAN computer code (Geelhood, Luscher, and Beyer 2011b) to evaluate three of the tests in the IFA-650 series, namely, tests 2, 3 and 4 (Ek 2005a; Ek 2005c; Ek 2005b; Kekkonen 2007). The results of our computations are compared with measured data for the following parameters: (i) Cladding temperature as a function of time; (ii) Fuel rod pressure as a function of time; (iii) Cladding diameter at rupture versus axial position of rod; (iv) Peak cladding temperature at rupture; and (v) Maximum outer surface cladding oxide layer thickness after LOCA transient (test 2). Two versions of FRAPTRAN-1.4 was used in our evaluations for the sake of benchmarking; namely FRAPTRAN-QT1.4b (Jernkvist 2010) adapted in Quantum Technologies and FRAPTRAN-GENFLO developed by Technical Research Centre of Finland (VTT), which connects FRAPTRAN-1.4 with the thermal-hydraulic program GENFLO (Miettinen and Hämäläinen 2002). Even in the FRAPTRAN-QT1.4b computations of the IFA-650 tests, we have used the thermal-hydraulic boundary conditions calculated by FRAPTRAN-GENFLO. That is, we have employed the FRAPTRAN-GENFLO calculated time variations of the coolant pressure and cladding outer surface temperatures as prescribed boundary

conditions in FRAPTRAN-QT1.4b.

The FRAPTRAN-QT1.4b code has recently been verified (Manngård, Jernkvist, and Massih 2011) against high temperature cladding burst data obtained from the REBEKA LOCA experiments (Erbacher, Neitzel, and Wiehr 1990). The IFA-650.2 test has also been previously analyzed by us using different versions of the FRAPTRAN code (Manngård 2011). These calculations were performed with the standard (default) input option for plenum temperature, whereas the plenum temperature in the current analyses of the IFA-650 tests is either based on GENFLO calculations or derived from measured quantities. The standard option overestimates the plenum temperature in the Halden IFA-650 type test fuel rods, thereby leading to an overestimation of the rod gas pressure during the heat-up phase of LOCA transient (Geelhood, Luscher, and Beyer 2011c). The FRAPTRAN-QT1.4b calculations of REBEKA tests (Manngård, Jernkvist, and Massih 2011) and those performed within the aforementioned IFA-650.2 analysis (Manngård 2011) used the stress-base failure criterion by (Erbacher, Neitzel, Rosinger, Schmidt, and Wiehr 1982), whereas the average (best-estimate) stress-base criterion by (Rosinger 1984) is applied for the IFA-650 tests in the present work.

The report is organized as follows. Section 2 provides brief descriptions of the Halden IFA-650 tests considered in our evaluation. Here, we also include fuel rod design data, used as input to the codes, and a summary of the main results of the experiments. The versions of the employed computer codes are briefly described in section 3. The fuel rod calculations of the tests are presented in section 4, in which also the results of the calculations are compared with measured values. Input options to the codes are specified in Appendix A. Finally in section 5, we end the report by making some concluding remarks.

2 Halden IFA-650 experiments

The Halden IFA-650 series of tests refer to fuel rod experiments performed in the Halden boiling heavy-water reactor (HBWR) under simulated loss-of-coolant accident (LOCA) conditions. The test fuel rods used in experiments 2, 3 and 4, which are analyzed in this report, are described briefly in the sequel. The data for these test rods are summarized in table 1. A schematic drawing of the IFA-650 test rig is shown in figure 1. The test rod is placed in the center of the rig and surrounded by an electrical heater inside the flask. The heater is part of a flow separator, which separates the space into a central channel adjacent the fuel rod and an outer annulus. The heater was used to simulate the isothermal boundary conditions, i.e. the heat dissipated from the nearby fuel rods during a LOCA. Cladding temperature is affected by both the fuel rod and the heater power. The rod power is controlled by varying the reactor power. The inner/outer diameters of the heater and pressure flask are 20/26.2 mm and 34/40 mm, respectively. The IFA-650 test rig instrumentation for the actual tests consisted of 2-4 cladding surface thermocouples, a fuel rod elongation detector, a fuel rod pressure transducer, two fast response cobalt neutron detectors and three vanadium neutron detectors, two heater surface thermocouples and coolant thermocouples at the inlet and the outlet of the rig. Test 3 and 4 were also equipped with thermocouples at the axial level of the rod upper plenum volumes. Certain thermocouples (TCC) and their axial locations are summarized in table 2. The fuel pressure transducer (PF1) is connected to the top part of the test fuel rod. The temperature of the heater is measured by two embedded

thermocouples located axially at either side of the fuel stack at mid-level.

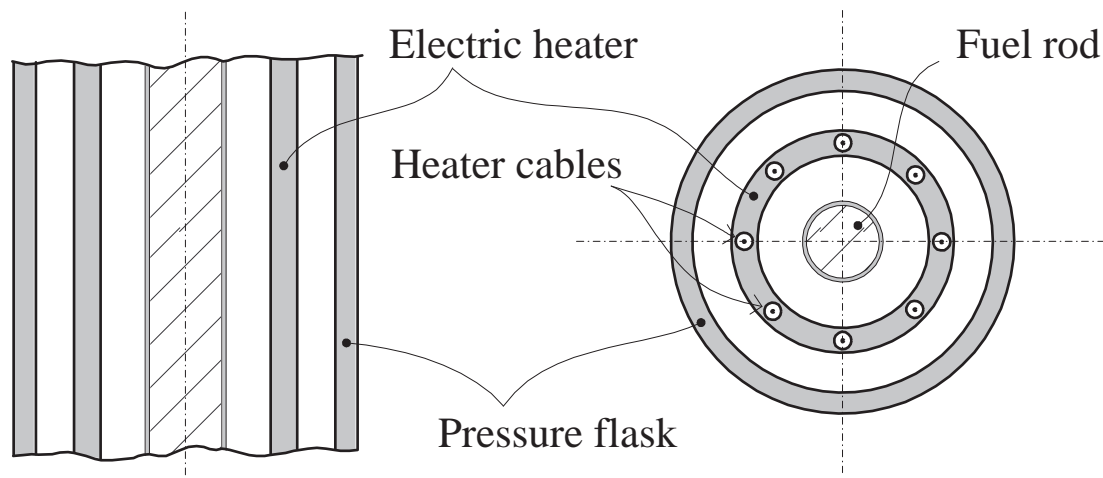


Figure 1: Schematic drawing of the IFA-650 test rig cross sections.

2.1 IFA-650.2

In the second experiment of this series, IFA-650.2 (Ek 2005a; Ek 2005c), a fresh (unirradiated) PWR UO_2 fuel rod (17×17 fuel assembly) with low-tin Zircaloy-4 cladding having outer diameter and wall thickness of 9.5 mm and 0.57 mm, respectively, was tested. The active length of the test fuel rod was 500 mm. The data for the rod in the IFA-650.2 experiment are summarized in table 1. The rod was pre-pressurized with helium to 4 MPa at room temperature. The IFA-650.2 test rig design and instrumentation are described in (Ek 2005a).

In the IFA-650.2 test, the LOCA simulation was initiated by a blowdown phase, during which the pressure in the coolant channel decreased from 7.0 to 0.4 MPa in about 35 seconds. After the blowdown, the heat-up period of the LOCA was simulated by turning on the electrical heater. The heater power was held at a constant value of 1.8 kW/m. Furthermore, during the test, the rod was kept at a small constant average nuclear power of 2.3 kW/m to provide suitable conditions for cladding deformation (ballooning) and oxidation. The axial rod power distribution produced by nuclear heating was roughly sinusoidal with a peaking factor of about 1.06 at the half-height position of fuel stack. During the heat-up phase the cladding was subjected to a temperature rise from 215 to 1050°C in about 200 seconds. Cladding rupture was detected inter alia by the cladding thermocouple and elongation (rod length change) signals at about 800°C, i.e. at about 100 s after initiation of the blowdown. The average cladding heating rate up to the instant of rupture was about 8.5°Cs⁻¹. A retardation of the heating rate (to around 5°Cs⁻¹) was observed in the cladding thermocouple temperature recordings just before the occurrence of rupture (rod failure). Post-test visual examination of the rod revealed that the fuel cladding had ruptured by an axial crack at the fuel rod peak power position. The average hoop strain prior to burst, obtained by measuring the diameter increase close to the burst opening was in the range of 35-40%. Over an axial distance of about 300 mm, including the burst area, the rod showed a noncircular diameter increase (Ek 2005a). The results obtained from IFA-650.2 are summarized in table 3.

Table 1: IFA-650 test rod data. Numerical values are those of the as-fabricated ones except burnup, cladding outer oxide layer thickness and cladding hydrogen content.

Test number		2	3	4
PELLET:				
Material		UO ₂	UO ₂	UO ₂
Diameter	mm	8.29	9.132*	9.13
Length	mm	8	11	11
Dishing		both ends	both ends	both ends
Dish depth	mm	0.20	0.28	0.25
Land width	mm	1.15	1.2	0.6
Density (UO ₂)	% of TD	95	94.8	95.2
U-235 enrichment in UO ₂	wt.%	2	3.5	3.5
CLADDING:				
Material		Low-tin [†] Zircaloy-4	DX ELS0.8b [‡]	DX Zr2.5Nb [#]
State		...	SRA ^b	SRA
Outer diameter	mm	9.5	10.735*	10.75
Wall thickness	mm	0.57	0.721	0.725
Outer oxide layer thickness (mean/max)	μm	...	24/27	10/11
Hydrogen content	ppm	...	250	50
FUEL ROD:				
Burnup	MWd/kgU	0 (fresh fuel)	81.9	92.3
Active length	mm	500	480	480
Total length of test rod	mm	1040	985	985
Radial pellet-clad gap	mm	0.035	0.0805*	0.085
Plenum volume	cm ³	15	21	21.5
Fill gas		He only	95%He+5%Ar	95%He+5%Ar
Fill pressure	MPa	4.0	4.0	4.0
Fabrication temperature	°C	25	25	25

* Actual value instead of nominal (unirradiated condition). [†] “Low-tin” refers to Sn content in the lower part of the range specified for Zircaloy-4 (1.2-1.7 wt.% Sn) according to ASTM R60804 specification. [‡] Zircaloy-4 cladding with 100 μm thick outer layer of Zr alloy with reduced tin content (0.8 wt.% Sn) relative to the base material. (DX=Duplex, i.e. dual-layer material, ELS=Extra Low Sn) [#] Zircaloy-4 cladding with 150 μm thick outer layer of Zr alloy with 2.5 wt.% Nb. ^bSRA = stress relief anneal.

2.2 IFA-650.3

In test three, IFA-650.3 (Ek 2005b), an irradiated PWR UO₂ fuel rod with Zircaloy-4 base duplex (double layer) cladding (16 × 16 fuel assembly) with outer diameter and wall thickness of 10.735 mm and 0.721 mm, respectively, was tested. The outer cladding layer with a thickness 0.15 mm had a reduced tin content relative to the base material (0.84 wt.% versus 1.48 wt.%). The test rod was re-fabricated from a section taken between the second and third spacer grid of a full-length rod pre-irradiated in a commercial PWR to a rod burnup of 82 MWd/kgU. The active length of the re-fabricated test fuel rod was 480 mm. The base irradiation of the full-length rod comprised 6 reactor cycles corresponding to 1994 effective full power days (EFPD). The cycle average base power history is depicted in figure 2. The

Table 2: Axial positions (in mm) of thermocouples (TCC) used in the IFA-650 test rigs. The axial positions are relative to the fuel stack bottom end.

Test number	2	3	4
Thermocouples:			
cladding	100 (TCC1)	100 (TCC1)	400 (TCC1)
	400 (TCC2)	400 (TCC2)	400 (TCC2)
	400 (TCC3)
	400 (TCC4)	400 (TCC4)	...
coolant/channel	...	570 (TCC3)	670 (TCC4)
plenum gas	678 (TCC3)

average linear power densities during the cycles were 37.0, 27.5, 21.5, 19.5, 18.0 and 18.0 kW/m, respectively. The data for the rod used in the IFA-650.3 experiment are summarized in table 1. The IFA-650.3 test rig design and instrumentation are described in (Ek 2005b). The test rod was filled with a gas mixture consisting of 95 vol.% argon and 5 vol.% helium to a pressure of 4 MPa at room temperature. Argon was selected to mimic the fission product gases, while a small amount of helium was needed to leak test the rod. The rod plenum volume (free gas volume) was made sufficiently large in order to maintain stable pressure conditions until cladding burst.

At initiation of the heat-up phase, the heater power was turned on to a preset value of 1.5 kW/m which was reduced stepwise when approaching the target cladding temperature for the test (800°C). The final heater power at target was 0.7 kW/m. The fuel rod was kept at an average constant nuclear power of about 1.0 kW/m. The axial rod power profile was symmetric and slightly peaked in the middle (axial peak to average power ratio was ≈ 1.04 ; see figure 3). The intent cladding temperature of 800°C was attained at about 300 s after blowdown, and the hold time at the maximum temperature to reactor scram was ≈ 5 minutes. Cladding failure occurred ≈ 266 s after the blowdown at $\approx 780^\circ\text{C}$ as indicated by rod elongation, pressure and cladding temperature measurements as well as the gamma ray monitor on the blowdown line to the dump tank. The average temperature increase rate prior to the burst was 2.5°Cs^{-1} . Halden experimenters cooled the test rod by spraying (with water) after the cladding burst. The test was terminated by a reactor scram.

Cladding failure in the IFA-650.3 experiment was detected by a first fast drop in the rod pressure signal (PF1 recording) at 266-267 s (after the initiation of the blowdown) which was followed by a gradual decrease in pressure. Figure 4 shows the evolution of rod pressure after the start of the blowdown phase. The rod pressure signal from the test shows a peak of 7.3 MPa between 245-250 s after blowdown. The average rod pressure from blowdown to the point of rupture is roughly 6.6 MPa. After cladding rupture, and after first fast pressure drop, the rod pressure fell rather slowly indicating that the rod failed by a relatively small crack rather than by a large burst. It took over one minute for the rod pressure to fall below 1 MPa after the instant of rupture. At this point (1 MPa) the expansion of the pressure bellows was mechanically stopped, thereby terminating the rod pressure measurement. The pressure signal stabilized at a constant level of 0.8 MPa. In effect the rod pressure continues to fall down to the rig pressure of about 0.4 MPa. A summary of IFA-650.3 test results is given in table 3.

Table 3: Summary of measured results from the considered IFA-650 tests.

Test number	2	3	4
Time to rupture after start of blowdown, s	99	267	336
Axial location ^a of rupture, mm	195-230	100	175-249
Axial length of rupture (crack), mm	35	...	74
Max. lateral width of crack opening, mm	20	...	8
Av. rod pressure from blowdown to rupture, MPa	6.6 ^b	6.6 ^b	6.5 ^b
Rod pressure at rupture, MPa	5.6 ^b	7.1 ^b	7.1 ^b
Cladding diameter increase ^c close to rupture area, %	35-40	...	35-40
Max. cladding diameter increase ^d in rupture area, %	90	<10	65
Cladding-heater mechanical interference at rupture (Yes/No)	...	No	Yes
Cladding temperature at start of heat-up, °C	220	200	190
Cladding temperature at rupture, °C	800	780	785
Av. cladding temperature increase rate during heat-up until rupture, °Cs ⁻¹	8.5	2.5	2.0
Typical cladding azimuthal temperature variation during heat-up until rupture, °C	5 ^f
Max. measured cladding temperature:			
upper thermocouple position, °C	1036	822	785
lower thermocouple position, °C	1091	837	...
Cladding inner/outer surface oxide layer, μm	40-50	...	2-3/10-13

^a From bottom end of fuel stack. ^b To obtain the differential pressure across the cladding wall, the rod pressure value shall be subtracted by the coolant channel pressure (0.4 MPa) after blowdown. ^c Estimated from measured diameter increase ΔD with respect to initial cladding outer diameter D_0 by $\Delta D/D_0 \times 100\%$.

^d Estimated from measurements of circumferential length L of fractured cladding. The diameter increase is obtained by relating L with initial cladding circumference L_0 by $L/L_0 \times 100\%$. ^f Estimated from upper thermocouple measurements (TCC2,-3 and -4).

2.3 IFA-650.4

In test four, IFA-650.4 (Kekkonen 2007), an irradiated PWR UO₂ fuel rod with Zircaloy-4 base duplex cladding with outer diameter and wall thickness of 10.75 mm and 0.725 mm, respectively, was tested. The original fuel rod was of the same design as that of the aforementioned IFA-650.3. The test rod was re-fabricated from a section taken between the fifth and sixth spacer grids of a full-length rod pre-irradiated in a commercial PWR to a rod burnup of 92 MWd/kgU. The active length of the re-fabricated fuel rod was 480 mm. The base irradiation of the full-length rod comprised 7 cycles corresponding to 2305 effective full power days. The cycle average base power history is depicted in figure 2. The average linear power densities during the cycles were 33.5, 27.5, 30.0, 19.0, 18.0, 17.0 and 16.0 kW/m, respectively. The data for the rod used in the IFA-650.4 experiment are summarized in table 1. The IFA-650.4 test rig design and instrumentation are described in (Kekkonen 2007). The test rod was filled with a gas mixture consisting of 95 vol.% argon and 5 vol.% helium to a pressure of 4 MPa at room temperature. Argon was used to mimic the fission product gases, while a small amount of helium was needed to leak test the rod. The rod plenum volume (free gas volume) was made sufficiently large in order to maintain stable pressure conditions until cladding burst.

At the start of the blowdown the linear heat generation rate of the fuel rod was 0.93 kW/m and that of the heater 1.5 kW/m. Taking into account the excess decay heat, the fuel linear heat rate was close to 1.0 kW/m. The heater power was kept constant during the heat-up stage. The axial rod power profile was symmetric and slightly peaked in the middle (axial peak to average power ratio was ≈ 1.05 ; see figure 3). After blowdown, the intent cladding temperature of 800°C was attained, and the hold time was ≈ 5 minutes (from burst to scram). Cladding failure occurred ≈ 366 s after blowdown at $\approx 785^\circ\text{C}$ as indicated by rod elongation, pressure and cladding temperature measurements as well as the gamma ray monitor on the blowdown line to the dump tank. The average temperature increase rate prior to the burst was 2.0°Cs^{-1} . The test rod was cooled by spraying (with water) after the cladding burst. The test was terminated by a reactor scram.

Cladding began to deform when the rod pressure reached a peak value of about 7.1 MPa, $\approx 265 - 270$ s after blowdown. Then it slowly declined to 5.1 MPa at around 366 s. A large ballooning of cladding was verified with gamma scanning after the test. A rapid drop in pressure, indicating burst started at 366 s, where the rod pressure was dropped in 2 s from 5.1 MPa to 0.8 MPa. At this point the expansion of the pressure bellows was mechanically stopped, so that the pressure signal levelled off at about 0.8 MPa, although in reality the pressure would still keep falling until it would reach the rig pressure level 0.4 MPa. Figure 5 shows the rod internal pressure versus time after the blowdown. Various stages of the test (ballooning, burst, spraying, and scram) are also demarcated in this figure. A summary of IFA-650.3 test results is given in table 3. Spraying of the rod started 230 seconds after the burst. The first spray pulse was longer 12 s (0.5 s pulses every 20 seconds) and the cooling effect of the spray was seen upon temperature drop on the cladding from thermocouples. The heater power was kept constant throughout the test and reduced once at about 150 s after the burst. The heater was switched off 35 s after starting the spray. Shortly after (15 s), the test was terminated by a reactor scram. At the end of the cooling period one longer spray pulse was applied to enhance the cooling. After the test was ended, the rig was filled with helium.

One important feature of the IFA-650.4 test was an occurrence of fuel relocation during the test. More specifically, as a consequence of cladding ballooning and burst in IFA-650.4, fuel pellets from the upper portion of fuel column stack dropped into the ballooned region. It was observed (Kekkonen 2007) that about 190 mm of the original pellet stack was missing from the top part of the fuel column, which had dropped to the 60 mm long ballooned region at the mid-height of the rod, i.e., between an elevation of ≈ 1190 mm and ≈ 1250 mm. In the ballooned region, the rod diameter had uniformly increased by $\approx 50\%$ from the original value. Moreover, it was observed that some fuel pellets had moved out of fuel rod through the opening in the cladding, confirming that cladding burst had occurred.

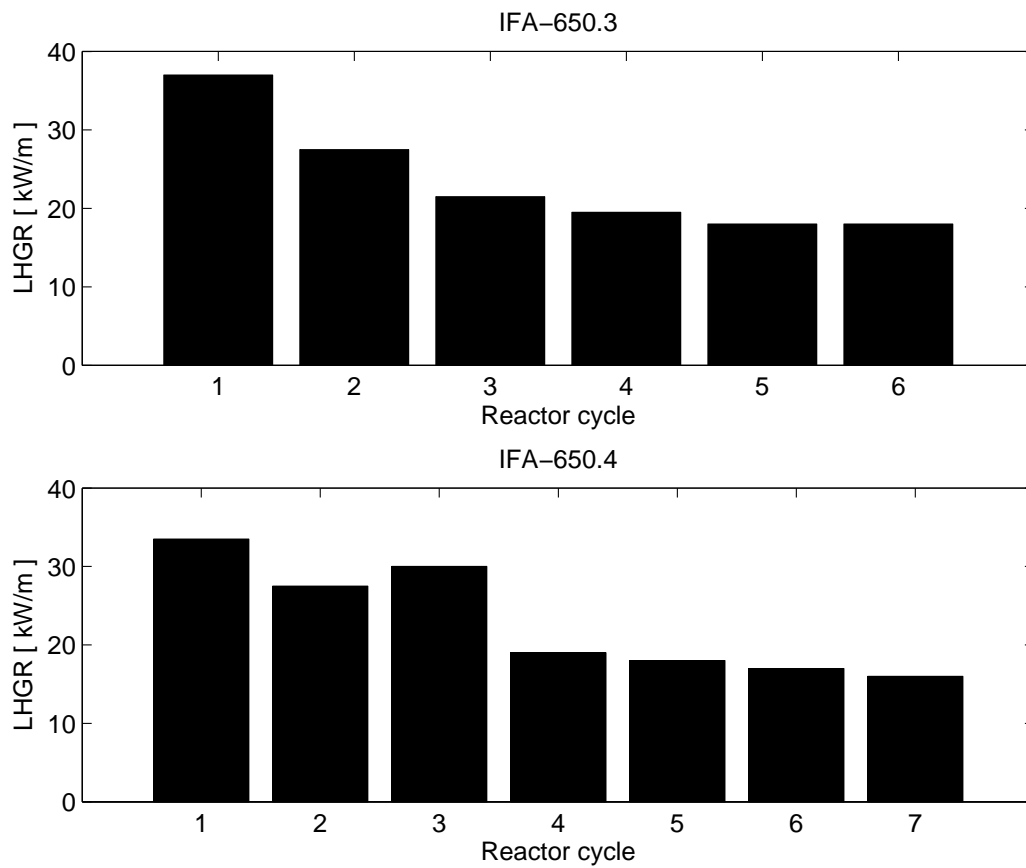


Figure 2: Cycle average base power history experienced by IFA-650.3/4 test fuel rods in a PWR. Linear heat generation rate versus reactor cycle (Ek 2005b; Kekkonen 2007).

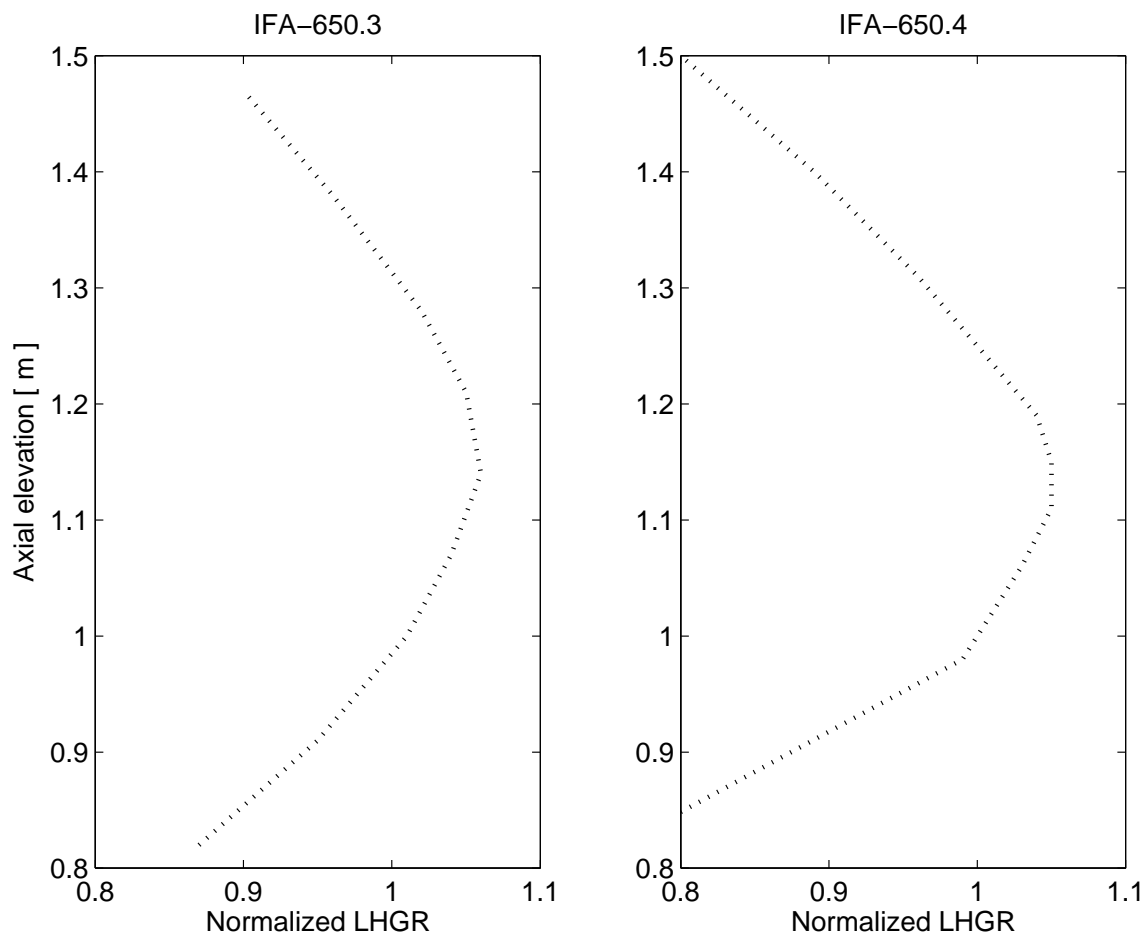


Figure 3: Axial power distributions produced by nuclear fission in the IFA-650.3/4 test fuel rods in the Halden reactor. Axial elevation versus normalized linear heat generation rate, adapted from (Ek 2005b; Kekkonen 2007). The lower end of the fuel stack is located at the axial elevation of 0.9 m.

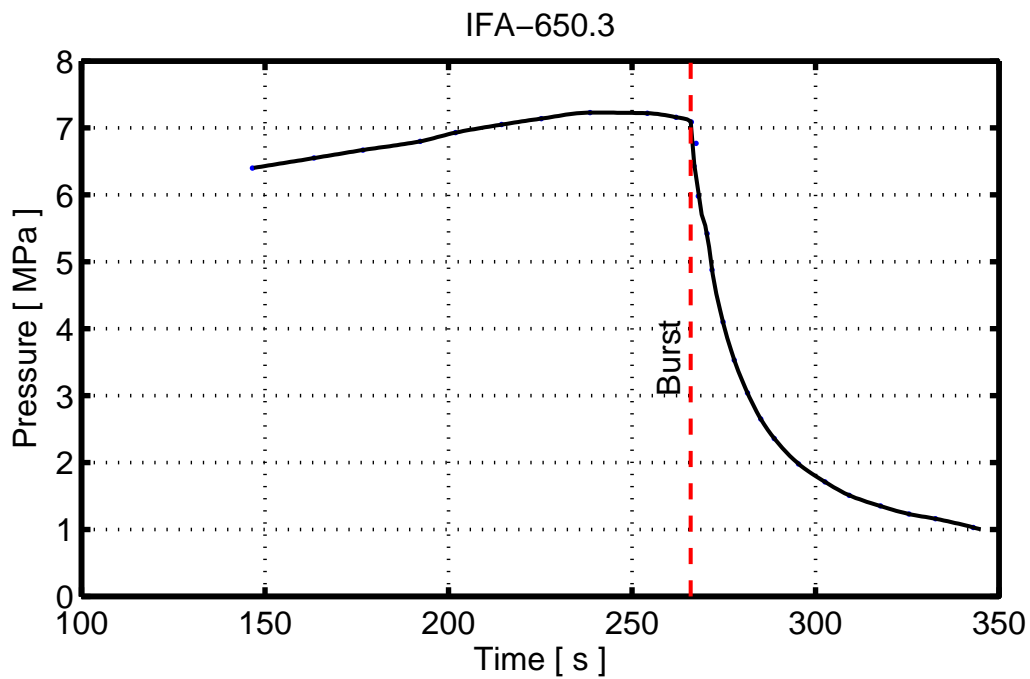


Figure 4: Measured rod pressure versus the time after the start of blowdown for IFA-650.3 rod in the Halden reactor. The vertical dash line indicates cladding burst (266-267 s), adapted from (Ek 2005b).

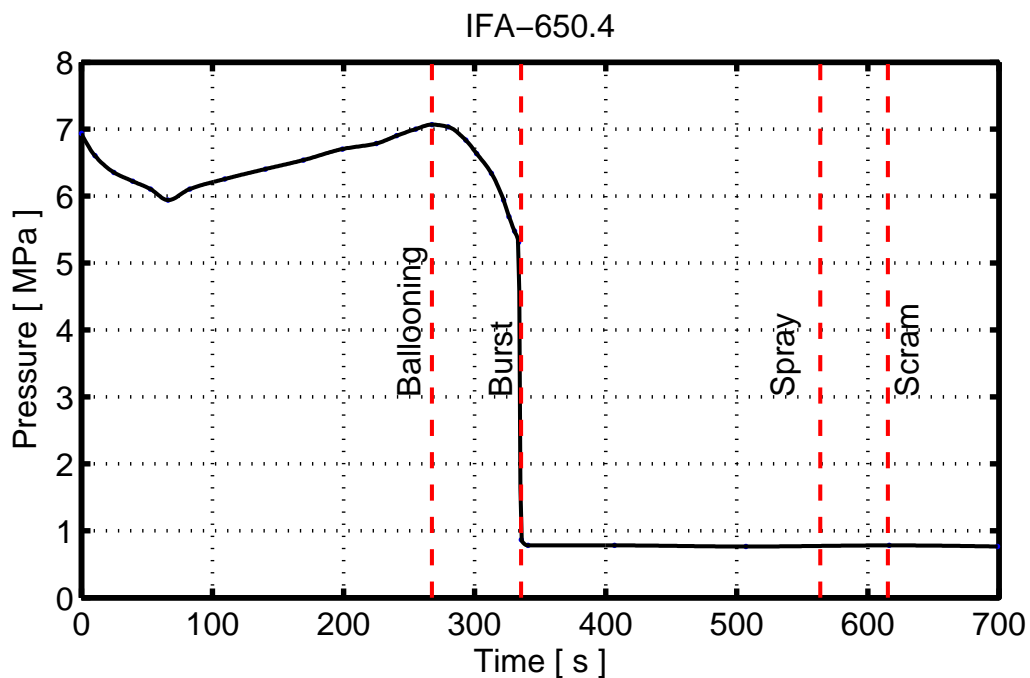


Figure 5: Measured rod pressure versus the time after the start of blowdown for IFA-650.4 rod in the Halden reactor, adapted from (Kekkonen 2007).

3 Computer codes

For the analysis of the Halden experiments considered in this report, we have utilized two variants of the computer program `FRAPTRAN-1.4`, namely, (i) `FRAPTRAN-QT1.4b` comprising an implementation of the model presented in (Manngård and Massih 2011) in `FRAPTRAN-1.4`, and (ii) `FRAPTRAN-GENFLO` developed by Technical Research Centre of Finland (VTT), which connects `FRAPTRAN-1.4` with the thermal-hydraulic program `GENFLO` (Miettinen and Hämäläinen 2002). Brief descriptions of these codes and appropriate references to their detailed accounts are given below.

The code `FRAPTRAN` (Fuel Rod Analysis Program Transient) simulates the light water reactor fuel thermal-mechanical behaviour when power and/or the coolant boundary conditions are rapidly changing (Geelhood, Luscher, and Beyer 2011b). More specifically, the code computes fuel rod attributes, such as fuel and cladding temperatures, cladding elastic and plastic strains, cladding stresses, fuel rod internal gas pressure, etc. as a function of irradiation time. `FRAPTRAN` affords a best-estimate code for analysis of fuel response to postulated accidents such as LOCA and interpreting experiments simulating such accidents. The `FRAPTRAN-1.4` code assessment, that is, comparison between code computations and data from selected integral irradiation experiments and post-irradiation examination programs is documented by (Geelhood, Luscher, and Beyer 2011c). The standard models and modelling options available in `FRAPTRAN-1.4` are described in (Geelhood, Luscher, and Beyer 2011b). The models implemented in the version 1.4 of `FRAPTRAN` can be used with the finite element based solution module of the code developed by (Knuutila 2006). Fuel rod variables that are slowly varying with time (burnup), such as fuel densification and swelling, and cladding irradiation creep and growth, are not calculated by `FRAPTRAN`. But, the state of the fuel rod at the time of a transient, which depends on those variables can be read from a file generated by the companion steady-state code `FRAPCON-3.4` (Geelhood, Luscher, and Beyer 2011a).

The `FRAPTRAN-QT1.4b` computational method is similar to that described in (Manngård and Massih 2011) with some extensions, modifications and adaption to an integral fuel rod modelling code (Jernkvist 2010). The main quantities calculated by the method are (i) oxygen parameters, which can be either the oxygen concentration picked up by the cladding during the oxidation process, the oxide layer thickness, or the oxygen concentration in the cladding metal layer; (ii) the volume fractions of the α -Zr and β -Zr during the phase transformation; (iii) the cladding hoop strain due to creep; and (iv) a cladding burst stress criterion. All these quantities are coupled through a set of kinetic (differential) equations and the burst criterion, which are solved numerically. The `FRAPTRAN-QT1.4b` models are used with the aforementioned finite element solver of `FRAPTRAN-1.4`.

The `FRAPTRAN-GENFLO` code is a coupled reactor core thermal-hydraulic and fuel rod analysis package. `GENFLO` simulates the thermal-hydraulic behaviour of a fluid channel (surrounding a fuel rod) during LOCA conditions (Miettinen and Hämäläinen 2002). It includes models for reflooding and radiation heat transfer from fuel rod to the subchannel. `GENFLO` solves the coolant mass, momentum and energy conservation equations. It also computes the axial distributions of the fluid temperature and the fluid void fraction. The resulting fluid temperatures and heat transfer coefficients at each axial level for each time step are supplied to `FRAPTRAN`, which calculates temperatures and deformation of the

fuel pellets and cladding, including possible ballooning, see figure 6. The fuel specific computations are made by FRAPTRAN and the coolant specific calculations by GENFLO, for both codes. In the coupled code, FRAPTRAN is the main program calling GENFLO, which offers the thermal-hydraulic conditions for the entire subchannel. This computation is made only once for each time step, even if a number of iterations is done in FRAPTRAN during the time step. At the start, GENFLO is used to make a steady-state computation prior to any coupled code calculation. In the coupled code computation, FRAPTRAN dictates the time step length, typically 0.01-0.05 s, but the calculation is fast since GENFLO is non-iterative and effective numerical methods are applied (Daavittila, Hämäläinen, and Rätty 2005). The FRAPTRAN-GENFLO code package has been used in the past for the pre- and post test analyses of LOCA experiments performed at the Halden reactor (Miettinen, Stengård, and Kelppe 2004).

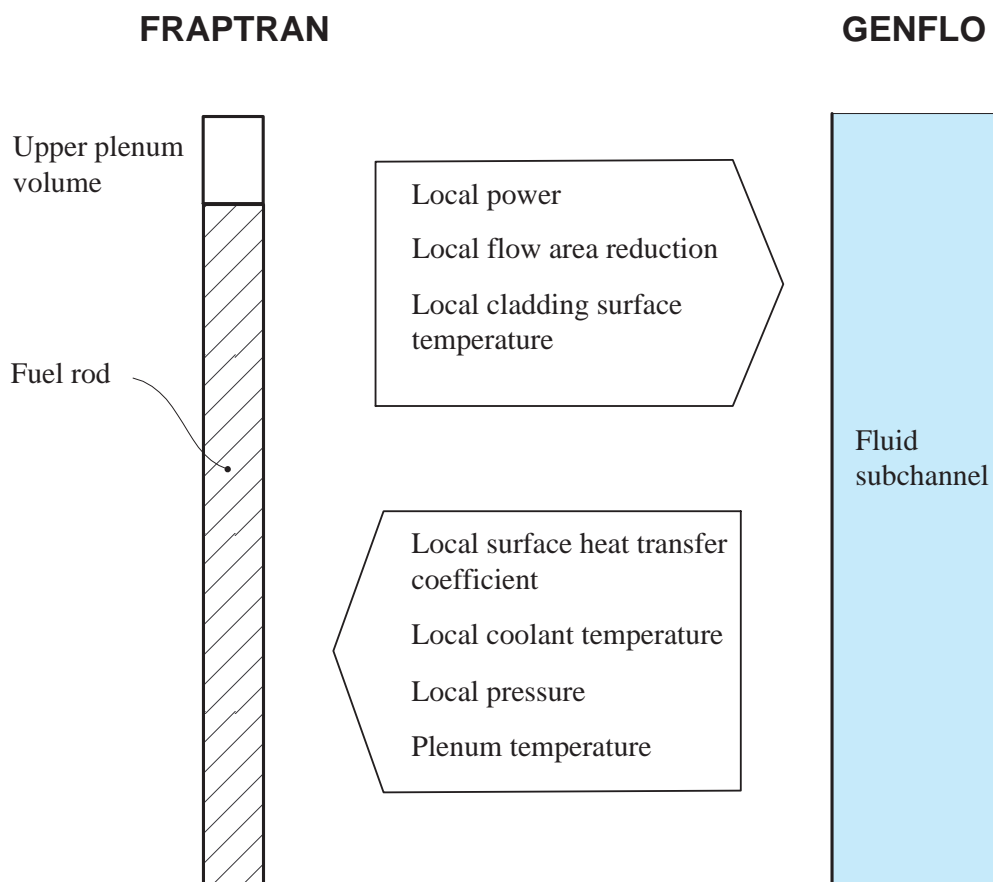


Figure 6: Coupling and data exchange in FRAPTRAN-GENFLO.

4 Calculations

Analyses of tests 2, 3 and 4 of the IFA-650 series using the `FRAPTRAN` code are presented in this section. The results from the calculations are compared with measured data for the following parameters:

- Cladding temperature as a function of time,
- Fuel rod pressure as a function of time,
- Cladding diameter at rupture versus axial position of rod,
- Peak cladding temperature at rupture and
- Maximum outer surface oxide layer thickness of cladding tube after LOCA transient (test 2).

The transient fuel rod calculations of the IFA-650 tests presented in this work involve two versions of the `FRAPTRAN` code described in the foregoing section. The `FRAPTRAN-QT1.4b` calculations of the IFA-650 tests use thermal-hydraulic boundary conditions calculated by `FRAPTRAN-GENFLO` code (Miettinen, Stengård, and Kelppe 2004). More precisely, we apply the calculated time variations of coolant pressure and cladding outer surface temperatures as prescribed boundary conditions for the cladding in the calculations with the `FRAPTRAN-QT1.4b` code. Moreover, the plenum temperature for the `FRAPTRAN-QT1.4b` calculations is either based on thermal-hydraulic calculations (`GENFLO`) or derived from measured quantities. For cladding failure, `FRAPTRAN-GENFLO` uses a strain-base cladding failure criterion, hoop strain versus burst temperature, whereas `FRAPTRAN-QT1.4b`, besides this option (not used here), employs a stress-base failure criterion, hoop stress versus burst temperature (cf. Appendix A).

The active length of the test fuel rods is divided into 10 axial segments, each of equal length. The cladding is structurally treated as a thin-walled tube, i.e. it is represented by a single finite element across its thickness. The input options defining the cladding models selected in the `FRAPTRAN` calculations, presented in this section, are summarized in Appendix A. The input instructions for the `FRAPTRAN-1.4` code are specified in (Geelhood, Luscher, and Beyer 2011b), whereas the additional input needed for use of the new cladding material models for LOCA analysis in `FRAPTRAN-QT1.4b` is described in (Jernkvist 2010). The time equal to zero ($t=0$) in the analyses refers to the start of blowdown. A constant time step length of 5 ms is used in the heat-up phase of the LOCA transient.

4.1 Fuel rod initial state

The `FRAPTRAN-GENFLO` calculations of preirradiated test rods, used in the IFA-650 experiments 3 and 4, are performed with burnup-dependent initial state calculated by the fuel rod steady-state behaviour code `FRAPCON-3.4`. Both calculations, by `FRAPCON` and `FRAPTRAN`, use 10 axial nodes to resolve fuel rod's active length. The nodal linear heat generation rates (LHGRs) for the `FRAPCON-3.4` calculations are obtained from the fuel rod base irradiation power histories by assuming a slightly skewed axial power distribution with maximum at the upper end of the rod. Moreover, the finite element (FE) based mechanical cladding module of the codes (Knuutila 2006) is applied consistently in both

the FRAPCON and FRAPTRAN calculations. Application of the FE analysis (FEA) model in FRAPCON produces an unformatted file for FRAPTRAN. Also, FRAPCON produces a formatted restart file for each time step, and the last time step information is used for FRAPTRAN. Because the rods are refabricated for tests 3 and 4 (from a full-length rod to a short test rod) a few modifications are made to the restart files. The amount of gas (mole) and its composition should correspond to the new rod filling. The new amount of gas is tuned by calculation of the first time step by FRAPTRAN at zero power and adjusted to get the correct initial pressure, i.e. the fill pressure of refabricated rod.

Fuel rod irradiation (power) history primarily influences fission product gas release, i.e. the gas composition in the rod and thereby the rod internal gas pressure. These quantities were reset to predefined values in the considered IFA-650.3 and -650.4 LOCA tests (see table 1) upon re-fabrication after their respective pre-irradiation. Moreover, fuel deformation and restructuring, and cladding deformation are chiefly burnup/exposure dependent, meaning that the details of power history have secondary effects on these quantities. Therefore, the effects of pre-irradiation simulations with FRAPCON on LOCA test simulations with FRAPTRAN should be slight.

The LOCA calculations of IFA-650 tests 3 and 4 with FRAPTRAN-QT1.4b are performed without FRAPCON-calculated initial fuel rod state, since verification calculations have shown that the impact of preirradiation on FRAPTRAN LOCA analysis results are small. Verification calculations were performed to check the influence of omitting the FRAPCON initialization (burnup-dependent rod state) on the final LOCA analysis results generated by the FRAPTRAN code. The differences between the two approaches, that is, LOCA analysis with and without FRAPCON initialization, were not significant despite that differences in calculated results existed. The conclusion of this verification is that LOCA analysis of a preirradiated (high burnup) test rod can be performed with sufficient accuracy by solely using FRAPTRAN, i.e. by treating the preirradiated rod in the same way as an unirradiated (fresh) fuel rod, but with a reset gas gap composition and rod internal pressure, and also by altered rod dimensions.

4.2 Coolant conditions and plenum temperature

The coolant pressure, cladding outside temperature and plenum temperature as a function of time for the IFA-650 tests 2, 3 and 4 are calculated by using FRAPTRAN-GENFLO. The results are presented below.

Coolant pressure: The time variations of calculated coolant pressure in the IFA-650 tests 2, 3 and 4, using FRAPTRAN-GENFLO, are plotted in figure 7. The depressurising of pressure vessel (flask) in the blowdown phase (from roughly 7 MPa down to rig pressure ≤ 0.4 MPa) in the tests takes about 35, 55 and 90 s, respectively. The transient LOCA calculations are carried out to 800 s after the initiation of the blowdown for IFA-650 tests 2 and 3, whereas test 4 is calculated to 400 s (dash-dot curve in figure 7). These times applied for the tests are sufficiently long for our purpose, since the main objective of our analyses is to compare the cladding deformation behaviour and rupture with that obtained experimentally. The calculated coolant pressure boundary conditions by FRAPTRAN-GENFLO are prescribed in the succeeding calculations by the FRAPTRAN-QT1.4b code.

Cladding outer temperature: The time variations of cladding outer surface temperature in the IFA-650 tests 2, 3 and 4, using FRAPTRAN-GENFLO, are plotted in figures 8a, 8b and 9, respectively. The calculated cladding temperatures are given in the thermocouple positions (TCC) used in the various tests. Note that the IFA-650.4 test (figure 9) is calculated to 400 s after the start of the blowdown ($t=0$ s). The calculated temperatures are in general in good agreement with the measured temperature recordings. The cladding temperature boundary conditions calculated by FRAPTRAN-GENFLO are prescribed in the calculations made by the FRAPTRAN-QT1.4b code.

Plenum gas temperature: The time variations of plenum gas temperature in the IFA-650 tests 2, 3 and 4, calculated by FRAPTRAN-GENFLO, are plotted as solid lines in figures 10, 11 and 12, respectively. The plenum gas temperature variations shown by the dashed lines in these three figures are prescribed in the FRAPTRAN-QT1.4b calculations. In figure 10 (IFA-650.2) the dashed line represents a simplified curve created from the calculated response (solid line), whereas the dashed lines in figures 11 (IFA-650.3) and 12 (IFA-650.4) represent measured quantities from the experiments. More specifically, the dashed line in figure 11 is the measured temperature variation of the fuel rod outer surface at an axial level that contains the plenum (TCC3 signal, see table 2). It should be mentioned that the TCC3 signal in figure 11 has been filtered from the background noise. The dashed line in figure 12 is the result of direct measurement of gas temperature by a thermocouple (TCC3 signal) located in the plenum volume of the rod, see table 2.

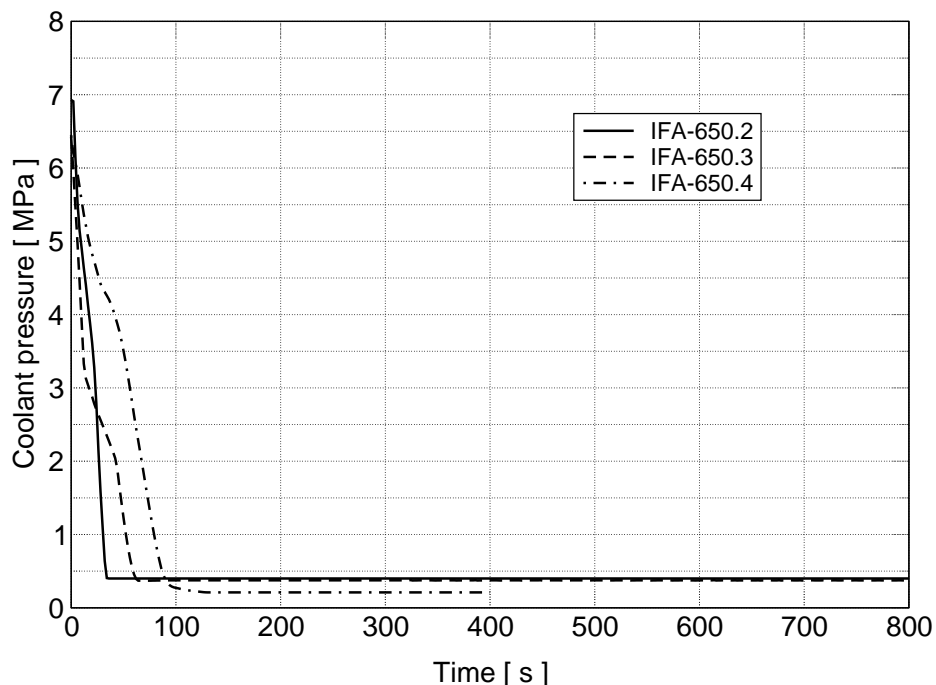
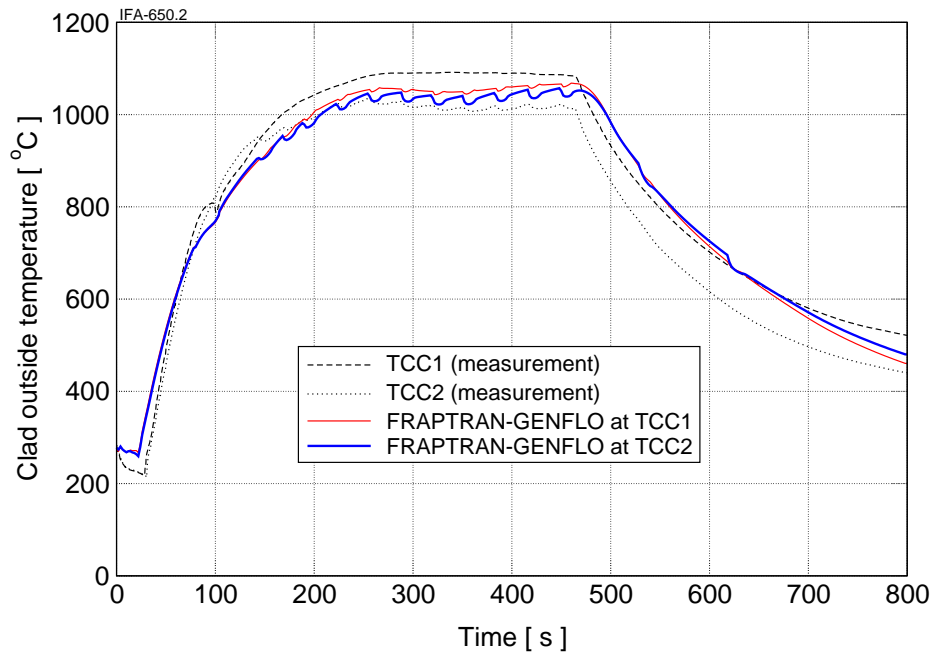
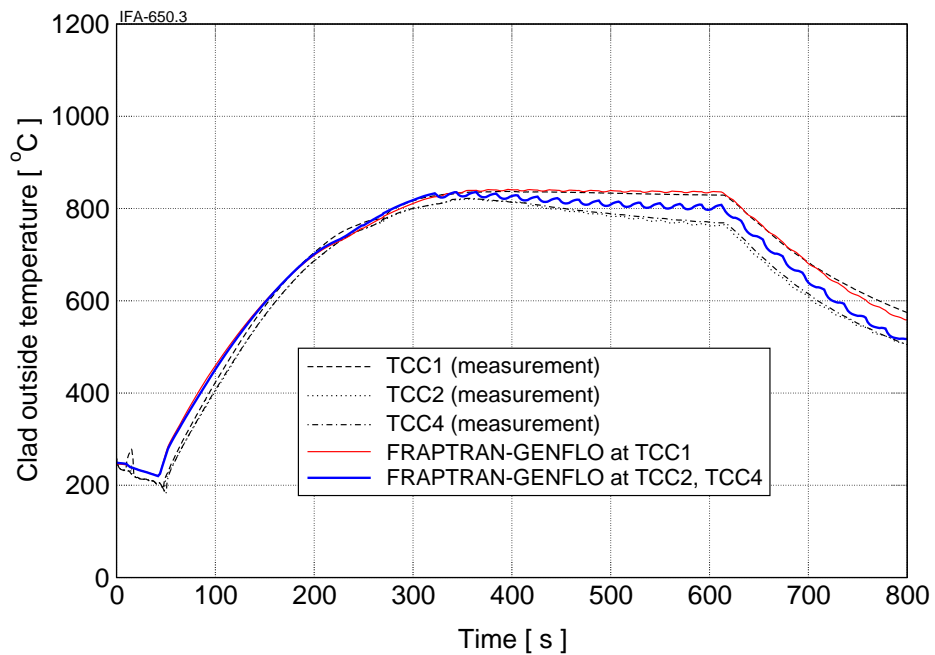


Figure 7: Calculated coolant pressure (rig pressure) variations with time for the IFA-650 tests 2, 3 and 4 using the FRAPTRAN-GENFLO code. The calculated coolant pressure boundary conditions by FRAPTRAN-GENFLO are prescribed in the calculations by the FRAPTRAN-QT1.4b code.



(a)



(b)

Figure 8: (a) IFA-650.2 (b) IFA-650.3 / Measured and calculated cladding outer surface temperatures in thermocouple positions. The axial positions of the cladding thermocouples (TCC) for the tests are given in table 2. The calculated cladding temperature boundary conditions by FRAPTRAN-GENFLO are prescribed in the calculations by the FRAPTRAN-QT1.4b code.

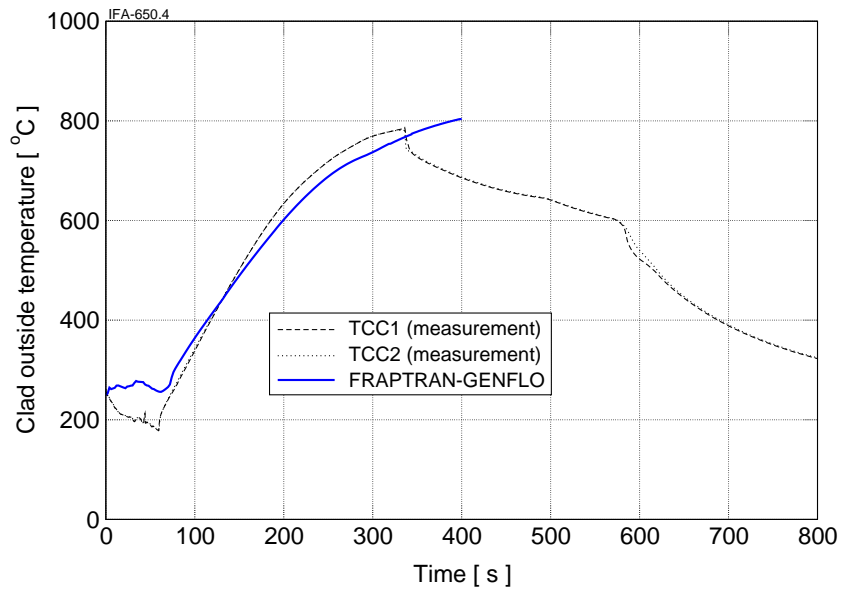


Figure 9: IFA-650.4 / Measured and calculated cladding outer surface temperatures in thermocouple positions. The axial positions of the cladding thermocouples (TCC) for the test are given in table 2. The calculated cladding temperature boundary conditions by FRAPTRAN-GENFLO are prescribed in the calculations by the FRAPTRAN-QT1.4b code.

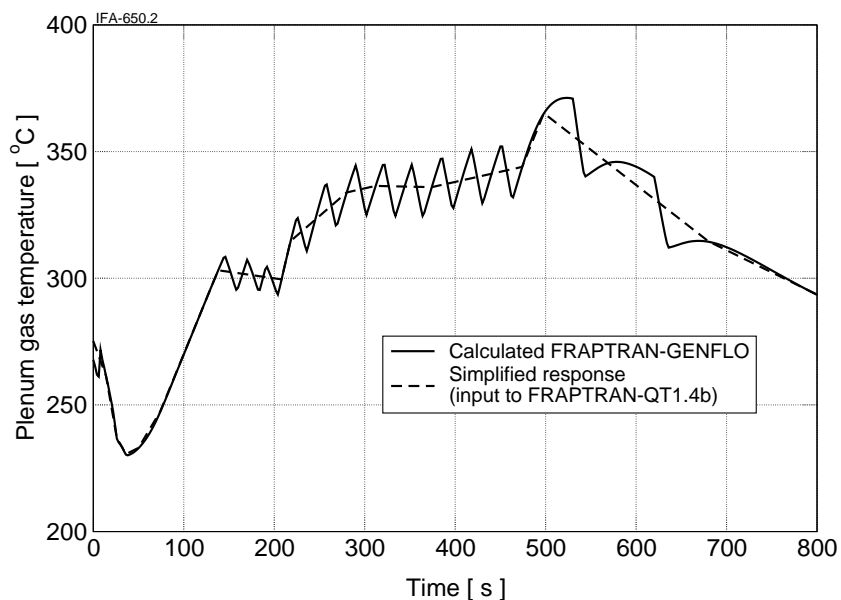


Figure 10: IFA-650.2 / Solid line; FRAPTRAN-GENFLO calculated time variation of plenum gas temperature. Dashed line; Simplified curve of the calculated response. The plenum gas temperature described by the dashed line is prescribed in the IFA-650.2 calculations by the FRAPTRAN-QT1.4b code.

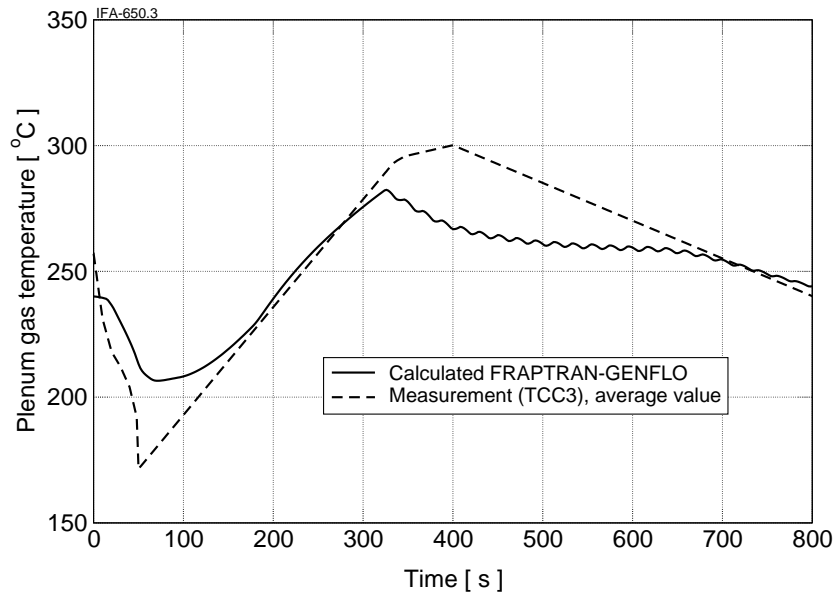


Figure 11: IFA-650.3 / Solid line; FRAPTRAN-GENFLO calculated time variation of plenum gas temperature. Dashed line; Measured temperature variation of the fuel rod outer surface at an axial level containing the plenum (TCC3 signal, filtered from noise). The temperature history described by the dashed line is used as prescribed plenum gas temperature in the IFA-650.3 calculations by the FRAPTRAN-QT1.4b code.

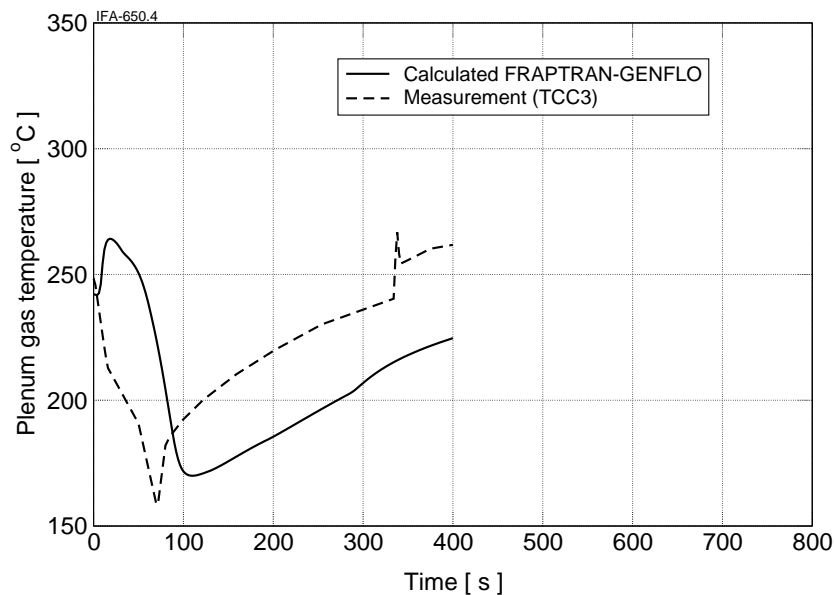


Figure 12: IFA-650.4 / Solid line; FRAPTRAN-GENFLO calculated time variation of plenum gas temperature. Dashed line; Measured plenum gas temperature variation (TCC3 signal). The measured temperature response is prescribed in the IFA-650.4 calculations using the FRAPTRAN-QT1.4b code.

4.3 Rod gas pressure

The rod gas pressure (plenum pressure) as a function of time for the IFA-650 tests 2, 3 and 4, calculated by FRAPTRAN-GENFLO and FRAPTRAN-QT1.4b, are compared with measurements in figures 13, 14 and 15, respectively. The rod gas pressure in these figures, calculated by FRAPTRAN-GENFLO, are shown as solid lines, whereas the FRAPTRAN-QT1.4b results are shown as dashed lines. The measured time responses of the rod pressure (PF1 signal) are plotted as dash-dot lines.

4.3.1 IFA-650.2

The cladding rupture measured in the experiment occurred 99 s after the start of the blow-down. At this moment the rod pressure dropped rapidly from 5.6 MPa to the rig pressure (0.4 MPa), although the pressure signal remained constant at 5.6 MPa, see figure 13 (Ek 2005a). The occurrence of cladding rupture obtained in the experiment is indicated by an asterisk in this figure. The calculated times to cladding rupture by the FRAPTRAN-GENFLO and FRAPTRAN-QT1.4b codes are 100 and 108 s, respectively. These rupture points are indicated by the cross symbol (\times) in figure 13. The calculated rod pressures at these instants, but just before cladding rupture, are 5.7 and 5.8 MPa, respectively.

4.3.2 IFA-650.3

The cladding rupture measured in the experiment occurred 266-267 s after the start of the blowdown. The measured rod pressure, just prior to cladding rupture in the experiment, was 7.1 MPa. After rupture, the gas pressure in the rod dropped, at first quite fast and then gradually with a decreasing rate with time; see the measured pressure signal shown by the dash-dot line in figure 14 (Ek 2005b). The course of events in the experiment is outlined in section 2.2. The times to cladding rupture calculated by the FRAPTRAN-GENFLO and FRAPTRAN-QT1.4b codes are 263 and 262 s, respectively (figure 14). The calculated rod pressures just prior to rupture are 5.7 and 5.8 MPa, respectively.

4.3.3 IFA-650.4

The fuel rod cladding in the experiment failed 336 s after the start of the blowdown. The measured rod pressure, shortly before the cladding rupture, was 7.1 MPa. Upon failure the rod pressure dropped rapidly down to the rig pressure. The test rod experienced large ballooning and cladding burst followed by a collapse of the fuel stack upper part into the burst area. The axial relocation of fuel material led to a dramatic shift in the distribution of fissioning power from the upper to lower end of the rod. The simulation of these phenomena is omitted in the current work since our main focus here is to evaluate cladding deformation and burst. The experiment is outlined in section 2.3. The times to cladding rupture calculated by FRAPTRAN-GENFLO and FRAPTRAN-QT1.4b are 338 and 332 s, respectively (figure 15). At these time instants (prior to rupture) the calculated rod pressures are 5.3 and 5.6 MPa, respectively.

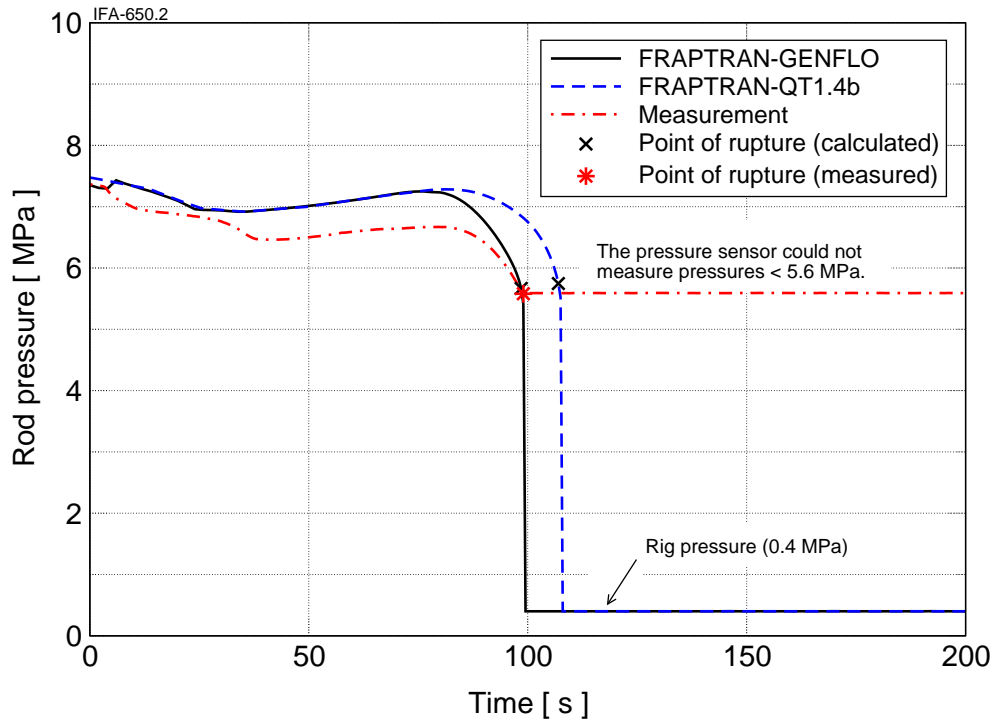


Figure 13: Rod gas pressure (plenum pressure) vs. time for the IFA-650.2 test, calculated by the FRAPTRAN-GENFLO (solid line) and FRAPTRAN-QT1.4b (dashed line) codes. Cladding rupture is calculated around 100 s after start of blowdown. The measured evolution of the rod pressure is shown by the dash-dot curve. In reality, the measured rod pressure reaches the rig pressure upon cladding rupture at 99 s (asterisk symbol). The pressure sensor could not measure pressures below 5.6 MPa (Ek 2005a).

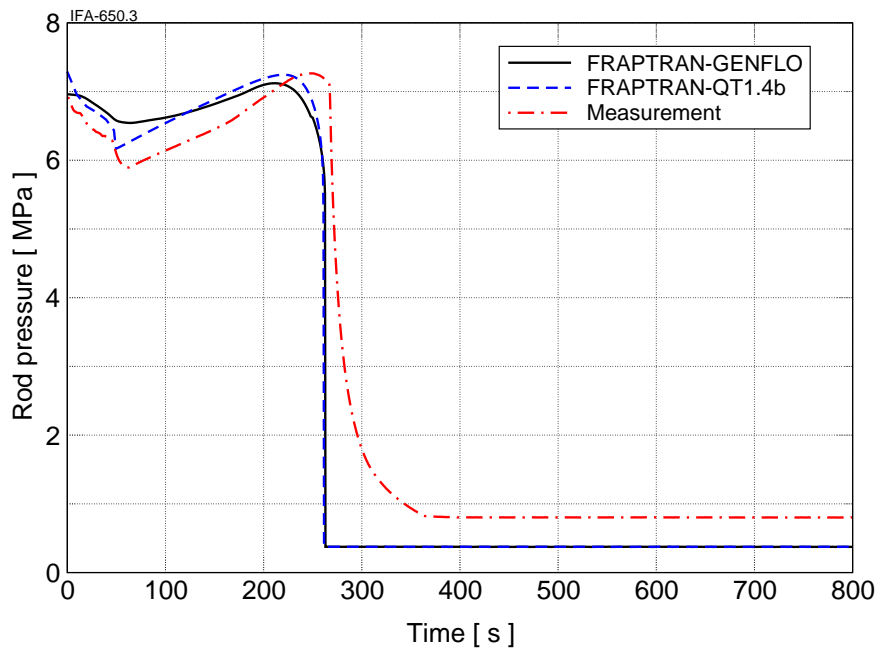


Figure 14: IFA-650.3 rod gas pressure variation with time calculated by the FRAPTRAN-GENFLO and FRAPTRAN-QT1.4b codes. The measured rod gas pressure variation during the transient is shown by the dash-dot curve (Ek 2005b).

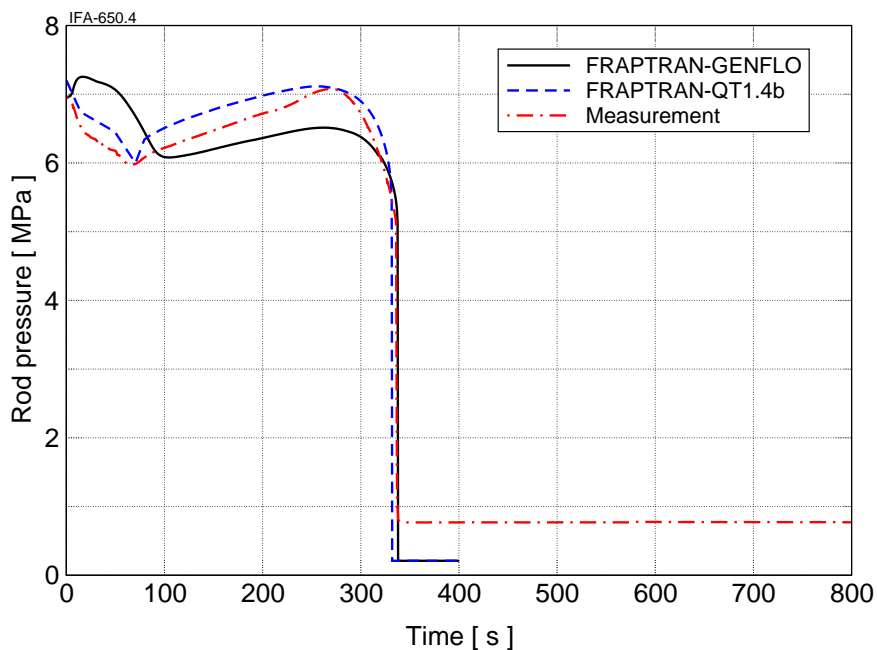


Figure 15: IFA-650.4 rod gas pressure variation with time calculated by the FRAPTRAN-GENFLO and FRAPTRAN-QT1.4b code. The measured rod gas pressure variation during the transient is shown by the dash-dot curve (Kekkonen 2007).

4.4 Cladding deformation and rupture

4.4.1 IFA-650.2

The calculated and measured cladding outer diameter profiles over the fuel stack region at burst are compared in figure 16. The two profiles plotted as solid and dashed lines are the results from calculations using the `FRAPTRAN-GENFLO` and `FRAPTRAN-QT1.4b` codes, respectively. The measured post-test cladding diameter profile for the IFA-650.2 rod, obtained as the average of three diametral trace measurements at 0, 45 and 135 degrees orientation along the rod (Ek 2005c), is given as dash-dot line in figure 16. The maximum measured diameter value at the open burst of the cladding is shown by an asterisk symbol.

Cladding rupture, by both codes, is calculated in axial node 5, i.e. in the rod's peak power position. This axial node corresponds to an axial elevation of 0.225 m from bottom end of the fuel stack, cf. figure 16. The calculated maximum diameters of the ruptured cladding are roughly 17 mm, whereas that obtained experimentally amounts to about 18 mm. The initial cladding diameter of the test rod was 9.5 mm. The calculated diameter profiles are, in general, in good agreement with measurements. The calculated deformations at rupture in the upper half of the rod match almost with measurements, whereas the diameter in the lower half of the rod is underestimated by about 1 mm relative to measurement. The differences between the calculations of cladding deformation made by `FRAPTRAN-GENFLO` and `FRAPTRAN-QT1.4b` for the IFA-650.2 test are small (figure 16). Also the calculated magnitudes of the cladding diameter at rupture (maximum values) as well as the rupture locations compare well with those of measurements (asterisk in figure 16).

4.4.2 IFA-650.3

The calculated and measured cladding outer diameter profiles over the fuel stack region at burst are compared in figures 17a and 17b for the IFA-650.3 test rod. The former figure compares the `FRAPTRAN-GENFLO` results with measurements and the latter the `FRAPTRAN-QT1.4b` results with measurements.

Post-test examination showed that the ruptured rod had developed uniform cladding deformation along the rod, but the maximum diameter increase was very small, only about 7% (at mid-stack height) (Ek 2005b). The burst location could not be found by visual inspection, but was instead determined by a leak test to be located in the lower thermocouple region. The measured diameter profile at rupture for the IFA-650.3 test rod is shown by the dash-dot line in figures 17a and 17b, representing the average of the four diametral trace measurements performed along the rod, that is at 0, 45, 90 and 135 degrees orientation (Ek 2005b). The burst location is indicated by an asterisk symbol in the plots, where the letter symbol "T" indicates thermocouple position. The cladding diameter measurements also revealed that local ballooning had started at the lower thermocouple position and at the middle of the rod when failure of the cladding occurred. However, in figures 17a-b we have omitted the abrupt variations in the diameter traces due to local ballooning at the lower thermocouple position and due to thermocouple clamp at the upper position (Ek 2005b). The details of the diameter measurement indicate that the general cladding deformation and ballooning in the middle of the rod proceeded as expected until the breach in the lower thermocouple area. The cladding deformations would certainly have been much larger if the rod had not failed prematurely. The grinding and welding operations to attach the ther-

mocouple to the rod may have weakened the cladding locally and thereby contributed to the early failure of the cladding in the experiment (Ek 2005b).

Cladding rupture, by both codes, is calculated to occur at the axial node 6, see the ring symbol in figures 17a-b. This axial node corresponds to an axial elevation of 0.264 m from bottom end of the fuel stack. The maximum cladding diameters at rupture for the IFA-650.3 experiment calculated by the `FRAPTRAN-GENFLO` and `FRAPTRAN-QT1.4b` codes, are 19.4 and 19.9 mm, respectively (see figures 17a-b). These maximum values are calculated at rod's peak power position. The initial diameter of the cladding in the test rod was 10.735 mm. The times to cladding burst calculated by the `FRAPTRAN-GENFLO` and `FRAPTRAN-QT1.4b` codes for the IFA-650.3 test rod are 263 and 262 s, respectively. The measured time to cladding rupture for the test was 267 s after the start of the blowdown. The calculated and measured rupture times are not directly comparable due to the apparently premature nature of the rod rupture in the experiment. For comparison, we have instead plotted the calculated diameter profiles at the time instant of 250 s at which the maximum diameter is close to that of the measured diameter profile. The calculated profiles at 250 s by `FRAPTRAN-GENFLO` and `FRAPTRAN-QT1.4b` are shown in figures 17a and 17b by the thin solid and thin dashed lines, respectively.

4.4.3 IFA-650.4

The calculated and measured cladding outer diameter profiles over the fuel stack region at burst for the IFA-650.4 test rod are compared in figure 18. The two profiles plotted by the solid and dashed lines are the results from calculations using the `FRAPTRAN-GENFLO` and `FRAPTRAN-QT1.4b` codes, respectively. The measured post-test cladding diameter profile outside the burst region (crack opening) for the IFA-650.4 rod is given by the dash-dot line. The diameter measurement reported by (Oberländer, Espeland, Solum, and Jenssen 2008) was performed at two different orientations along the rod, where the diameter profile for each orientation was determined by 13 sampling points (discrete diameter values). The diameter profile, representing the measurement in figure 18, is the average from these two orientations. The maximum cladding diameter just before burst in the experiment, plotted by an asterisk symbol in figure 18, corresponds to the maximum measured diameter increase of 65% (Oberländer, Espeland, Solum, and Jenssen 2008).

Cladding rupture, by both codes, is calculated in axial node 5, i.e. in the rod's peak power position. This axial node corresponds to an axial elevation of 0.216 m from bottom end of the fuel stack (figure 18). The maximum cladding diameters at rupture for the IFA-650.4 experiment calculated by the `FRAPTRAN-GENFLO` and `FRAPTRAN-QT1.4b` codes, are 19.9 and 20.1 mm, respectively, whereas that obtained experimentally amounts to about 17.7 mm (65% diameter increase). The initial cladding diameter of the test rod was 10.75 mm. We observe that the calculated maximum diameter at rupture by `FRAPTRAN-QT1.4b` is somewhat (0.1 mm) larger than the inner diameter of the heater (20 mm). However, since this possible interference with the heater is small, it is judged to be within the geometry tolerances of the rig equipment. We note that the cladding deformations, particularly outside the burst region, are generally underestimated by the codes compared with the measurements. More specifically, the calculated diameter profiles at the upper and lower halves of the test rod are underestimated by about 1-2 mm relative to measurements, whereas in the burst region (middle of rod) the calculated diameters are about 2 mm larger than the mea-

sured values, see figure 18. However, when evaluating the cladding deformations from the test it should be born in mind that the diameter measurement, especially outside the burst region, is insufficient. For example, there is no diameter measurement performed between the axial elevations of 0.30 and 0.45 m (figure 18). The differences in cladding deformations calculated by FRAPTRAN-GENFLO and FRAPTRAN-QT1.4b for the IFA-650.4 test are small.

The evaluation of the IFA-650 tests 2, 3 and 4 performed in this report is summarized in table 4.

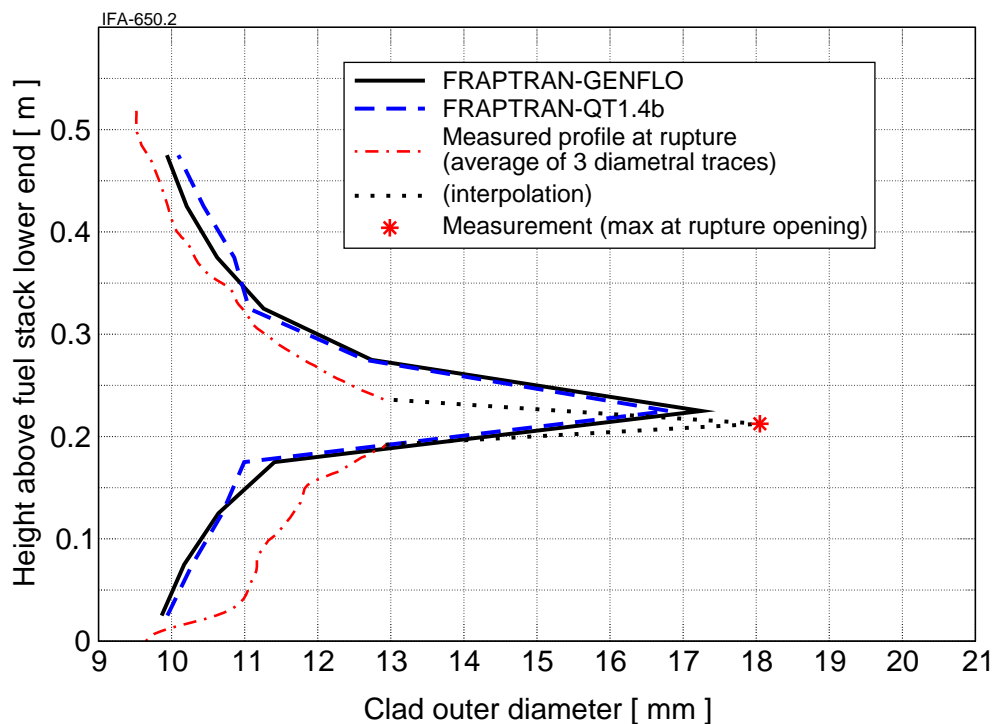
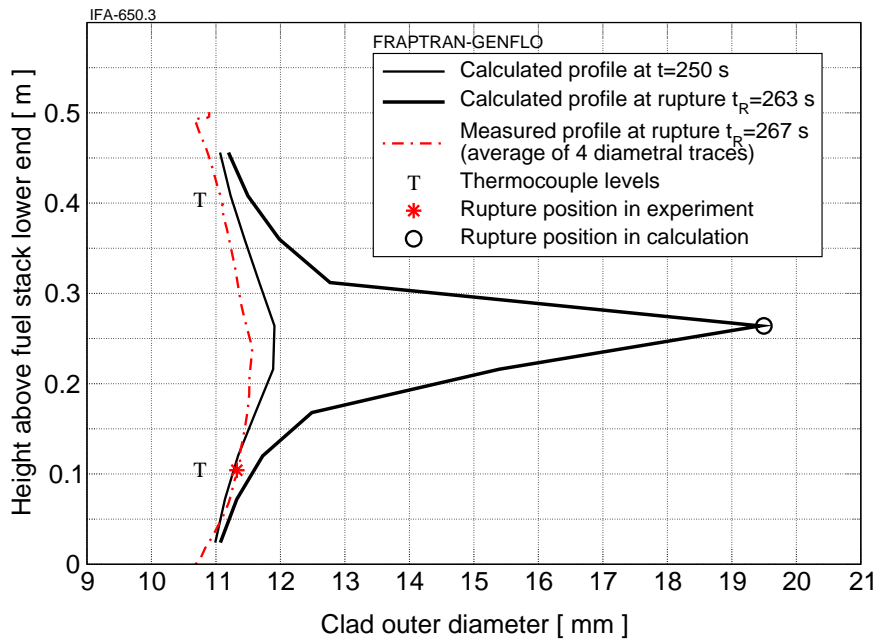
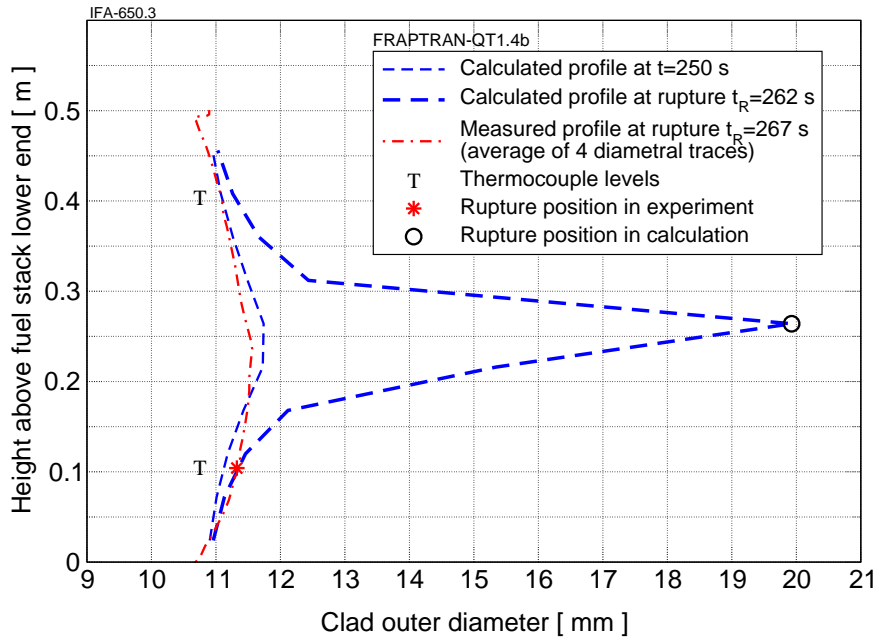


Figure 16: IFA-650.2 rod calculated and measured outer diameter profiles of cladding at burst. The two profiles shown by the solid and dashed lines represent the calculations made by FRAPTRAN-GENFLO and FRAPTRAN-QT1.4b, respectively. The corresponding measured diameter profile is shown by the dash-dot line (Ek 2005c) and maximum measured diameter by asterisk.



(a)



(b)

Figure 17: IFA-650.3 rod calculated cladding outer diameter at 250 s after blowdown and at burst using the (a) FRAPTRAN-GENFLO and (b) FRAPTRAN-QT1.4b codes. The measured post-test diameter profile along the rod (Ek 2005b) is shown by dash-dot line and measured rupture position by asterisk.

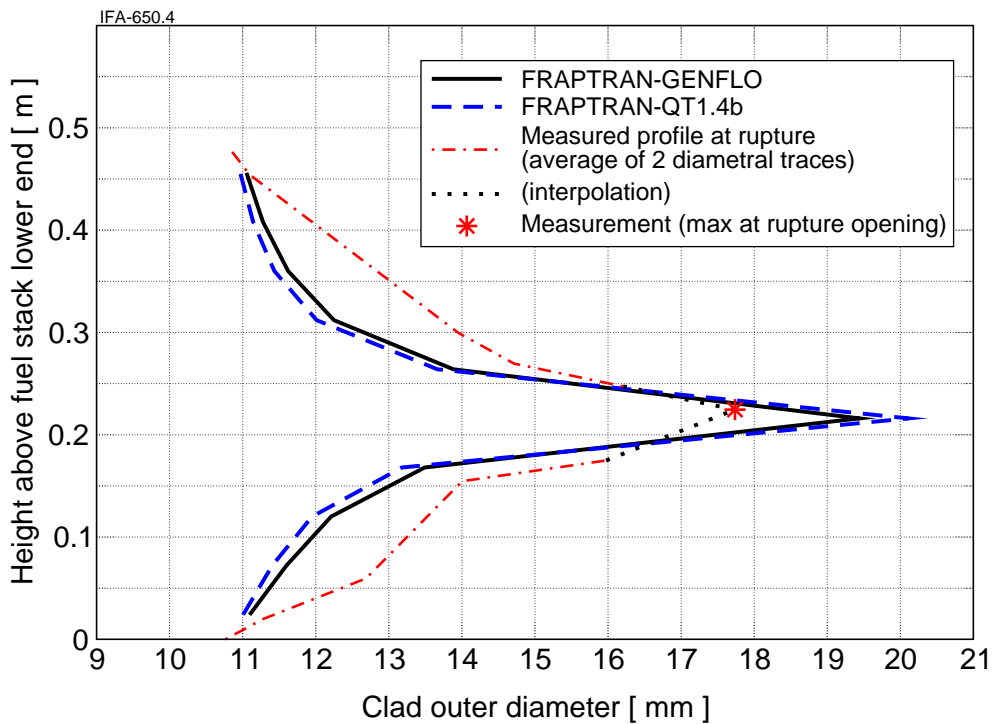


Figure 18: IFA-650.4 rod calculated and measured outer diameter profiles of cladding at burst. The two profiles shown by the solid and dashed lines, respectively, represent the calculation outcome by the FRAPTRAN-GENFLO and FRAPTRAN-QT1.4b codes. The measured diameter along the rod is shown by the dash-dot line (Oberländer, Espeland, Solum, and Jenssen 2008) and maximum measured diameter by asterisk.

Table 4: Comparison of calculated and measured results for the IFA-650 tests 2, 3 and 4.

Test/ Parameter	Calculation		Measurement
	1)	2)	
IFA-650.2/			
Time to cladding rupture, s	100	108	99
Rupture temperature, °C	773	806	800
Max. diametral cladding strain, %	82 ^b	76 ^b	90
Rod pressure at rupture, MPa	5.7	5.8	5.6
Outer surface oxide layer, μm thickness, μm	35	35	40-50
IFA-650.3/			
Time to cladding rupture, s	263	262	266-267
Rupture temperature, °C	796	797	780
Max. diametral cladding strain, %	81 ^b	86 ^b	<10
Rod pressure at rupture, MPa	5.7	5.8	7.1
Outer surface oxide layer, μm	10	10	...
IFA-650.4/			
Time to cladding rupture, s	338	332	336
Rupture temperature, °C	789	785	785
Max. diametral cladding strain, %	81 ^b	87 ^b	65
Rod pressure at rupture, MPa	5.3	5.6	7.1
Outer surface oxide layer, μm	10-13

¹⁾ FRAPTRAN-GENFLO

²⁾ FRAPTRAN-QT1.4b

^b Value obtained from the calculated increase of cladding outer diameter relative to initial cladding diameter of test fuel rod.

5 Concluding remarks

In this report, we have evaluated the Halden IFA-650 LOCA tests 2, 3 and 4 using two versions of the transient fuel rod code FRAPTRAN-1.4, namely FRAPTRAN-GENFLO and FRAPTRAN-QT1.4b. Since the former code is coupled to a thermal-hydraulic program (GENFLO), this capability is also utilized to prescribe the fuel rod boundary conditions for the FRAPTRAN-QT1.4b analyses reported here. For cladding mechanical calculations, the finite element method option of the codes is invoked. One point worthy for a remark is the computation of the gas temperature in the plenum region of the rod which accommodates most of the rod's void volume. The plenum gas temperature for FRAPTRAN-QT1.4b was either taken from the FRAPTRAN-GENFLO output or extracted from measurements. The fuel rod initial conditions after base irradiation (tests 3 and 4) for FRAPTRAN-GENFLO were precalculated using the steady-state fuel performance code FRAPCON-3.4. Since, however, our computations showed that the impact of preirradiation on FRAPTRAN LOCA analysis results are small, the FRAPTRAN-QT1.4b calculations were done without FRAPCON initialization.

In all three tests, the cladding failure occurred in the high α -Zr phase of the Zircaloy-4 material, i.e. at temperatures around and below 800°C, which is much lower than the

value (1204°C) set by the acceptance criteria. The calculated rupture temperatures for the tests agree well with measurements. Since cladding rupture in the tests occurs in the α -phase temperature range, the effect of the phase transition model in FRAPTRAN-QT1.4b does not come into play in the creep and rupture calculations. Computations made by both FRAPTRAN-GENFLO and FRAPTRAN-QT1.4b are, in general, in good agreement with the measured results regarding time to rupture and cladding deformation at rupture for tests 2 and 4. For test 3, in which the cladding failed prematurely at its lower end, the same amount of cladding deformation at rupture was calculated (by both codes) as for test 4. The two versions of code benchmark well with each other for the experiments evaluated in this report.

Acknowledgements

The work of T.M. and A.M. was supported by the Swedish Radiation Safety Authority (SSM) under the contract number SSM2011-2200/2030048-12. We thank Anna Alvestav (SSM) for her helpful comments. The VTT part of the work has been funded from the Finnish Research Programmes on Nuclear Power Plant Safety SAFIR2010 and SAFIR2014.

References

- Alam, T., M. K. Khan, M. Pathak, K. Ravi, R. Singh, and S. K. Gupta (2011). A review on the clad failure studies. *Nucl. Eng. Design* 241, 3658–3677.
- Daavittila, A., A. Hämäläinen, and H. Rätty (2005). Transient and fuel performance analysis with VTT's coupled code system. In *Mathematics and Computation, Supercomputing, Reactor Physics and Nuclear and Biological Applications*, Palais des Papes, Avignon, France, September 12-15, 2005. American Nuclear Society.
- Ek, M. (2005a). LOCA testing at Halden; The second experiment IFA-650.2. Technical Report HWR-813, Institutt for energiteknikk, OECD Halden reactor project, Halden, Norway.
- Ek, M. (2005b). LOCA testing at Halden, The third experiment IFA-650.3. Technical Report HWR-785, Institutt for energiteknikk, OECD Halden reactor project, Halden, Norway.
- Ek, M. (2005c). Minutes of the LOCA workshop meeting (FEB.-2005). Technical Report HWR-805, Institutt for energiteknikk, OECD Halden reactor project, Halden, Norway.
- Erbacher, F. J., H. J. Neitzel, H. Rosinger, H. Schmidt, and K. Wiehr (1982). Burst criterion of Zircaloy fuel claddings in a loss-of-coolant accident. In D. G. Franklin (Ed.), *Zirconium in the Nuclear Industry: Fifth Conference*, Volume ASTM STP 754, Philadelphia, USA, pp. 271–283. American Society for Testing and Materials.
- Erbacher, F. J., H. J. Neitzel, and K. Wiehr (1990). Cladding deformation and emergency core cooling of pressurized water reactor in a LOCA: Summary description of the REBEKA program. Technical Report KfK 4781, Kernforschungszentrum Karlsruhe, Karlsruhe, Germany.
- Geelhood, K. J., W. G. Luscher, and C. E. Beyer (2011a). FRAPCON-3.4: A computer code for the calculation of steady-state thermal-mechanical behavior of oxide fuel rods for high burnup. Technical Report NUREG/CR-7022, Vol. 1, US Nuclear Regulatory Commission.
- Geelhood, K. J., W. G. Luscher, and C. E. Beyer (2011b). FRAPTRAN 1.4: A computer code for transient analysis of oxide fuel rods. Technical Report NUREG/CR-7023, Vol. 1, US Nuclear Regulatory Commission.
- Geelhood, K. J., W. G. Luscher, and C. E. Beyer (2011c). FRAPTRAN 1.4: Integral assessment. Technical Report NUREG/CR-7023, Vol. 2, US Nuclear Regulatory Commission.
- Jernkvist, L. O. (2010). Implementation of models for cladding high temperature metal-water reactions, phase transformation, creep and failure in the FRAPTRAN-1.4 computer program. Technical Report TR10-005, Quantum Technologies AB, Uppsala, Sweden.
- Kekkonen, L. (2007). LOCA testing at Halden, The fourth experiment IFA-650.4. Technical Report HWR-838, Institutt for energiteknikk, OECD Halden reactor project, Halden, Norway.

- Knuutila, A. (2006). Improvements on FRAPCON3/FRAPTRAN mechanical modelling. Technical Report VTT-R-11337-06, VTT Technical Research Centre of Finland, Espoo, Finland.
- Manngård, T. (2011). Evaluation of the 2nd Halden IFA-650 loss-of-coolant accident experiment using the FRAPTRAN-1.4 and FRAPTRAN-QT1.4b computer codes. Technical Report TR11-001, Quantum Technologies AB, Uppsala, Sweden.
- Manngård, T., L. O. Jernkvist, and A. R. Massih (2011). Evaluation of loss-of-coolant accident simulation tests with the fuel rod analysis code FRAPTRAN-1.4. Technical Report TR11-008, Quantum Technologies AB, Uppsala, Sweden.
- Manngård, T. and A. R. Massih (2010). Modelling of nuclear fuel cladding under loss-of-coolant accident conditions. Technical Report TR09-008, Quantum Technologies AB, Uppsala, Sweden.
- Manngård, T. and A. R. Massih (2011). Modelling and simulation of reactor fuel cladding under loss-of-coolant conditions. *Journal of Nuclear Science and Technology* 48(1), 39–49.
- Massih, A. R. (2008). A model for analysis of Zr alloy fuel cladding behaviour under LOCA conditions. Technical Report TR08-007, Quantum Technologies AB, Uppsala, Sweden.
- Massih, A. R. (2009). Transformation kinetics of zirconium alloys under non-isothermal conditions. *J. Nucl. Mater.* 384, 330–335.
- Miettinen, J. and A. Hämäläinen (2002). GENFLO: A general thermal hydraulic solution for accident simulation. Technical Report 2163, VTT, Espoo, Finland.
- Miettinen, J., J.-O. Stengård, and S. Kelppe (2004). FRAPTRAN-GENFLO Calculations on the IFA-650 LOCA Test. In *Proceedings of Enlarged Halden Programme Group Meeting 2004, May 9-14 (HPR-362)*, Volume 2, Sandefjord, Norway.
- Oberländer, B. C., M. Espeland, N. O. Solum, and H. K. Jenssen (2008). LOCA IFA650-4: PIE of the high burnup (92 MWd/kgU) PWR segment. In *Proceedings of Enlarged Halden Programme Group Meeting 2008, May 9-14 (HPR-362)*, Number SESSION: F2/PAPER:7, Loen, Norway.
- Powers, D. A. and R. O. Meyer (1980, April). Cladding swelling and rupture models for LOCA analysis. Technical Report NUREG-0630, US NRC.
- Rosinger, H. E. (1984). A model to predict the failure of Zircaloy-4 fuel sheathing during postulated LOCA conditions. *J. Nucl. Mater.* 120, 41–54.
- USNRC (2011). *Appendix A to Part 50: General Design Criteria for Nuclear Power Plants*. US Nuclear Regulatory Commission.

Appendix A Input parameters for cladding models

The input parameters defining the cladding models and options applied in the FRAPTRAN calculations in section 4 of the report are described briefly in table A1, below. The default values are used for those options for which no values are given explicitly. The cladding model options are set in the \$model block of the FRAPTRAN input files. Further details on the input instructions are given in (Geelhood, Luscher, and Beyer 2011b) and (Jernkvist 2010).

Table A1: Definition of FRAPTRAN cladding models and options used in the calculations of the IFA-650 tests.

Program	Cladding model/ & suboptions	Description of selections
FRAPTRAN- GENFLO	mechan=1/ irupt=2 ruptstrain frcoef irefine=2	FE cladding mechanical model (FEA) Apply strain criterion for heating rates $\leq 10^\circ\text{C/s}$ from NUREG-0630 (Powers and Meyer 1980) to determine cladding failure. Maximum effective plastic+creep strain value (default=1.0) Coulomb coefficient of friction in pellet/cladding interface. (default=0.015) No mesh refinement in case of ballooning.
FRAPTRAN-QT1.4b	mechan=1/ icplcr=2 iccrp=1 irupt=5 icrup=2 plendef=0 ruptstrain=3.0 frcoef irefine=2	FE cladding mechanical model (FEA) Calculate only high-temperature creep deformation in cladding. Calculate mixed-phase creep rate by interpolation between single-phase creep rates. Apply average stress criterion by (Rosinger 1984) to determine cladding failure. Use temperature + phase composition for calculating cladding mixed-phase burst stress No creep deformation of gas plenum walls. Maximum effective plastic+creep strain value (default=1.0) Coulomb coefficient of friction in pellet/cladding interface. (default=0.015) No mesh refinement in case of ballooning.

Cladding models and options

FRAPTRAN-GENFLO: In the FRAPTRAN-GENFLO calculation with the FE cladding module, the rupture criterion option `irupt=2` is used. This option selects the burst hoop strain versus burst temperature correlation for cladding heating rates $\leq 10^\circ\text{C/s}$ (slow-ramp) defined in the NUREG-0630 document (Powers and Meyer 1980) as a rupture criterion. A similar burst correlation for $\geq 25^\circ\text{C/s}$ (fast-ramp) is also defined in (Powers and Meyer 1980), which can be selected in FRAPTRAN by setting `irupt=1`. However, since the

average heating rate during the heat-up phase in the considered IFA-650 tests is less than 10°C/s (table 3) we apply the former of these two burst options.

The GENFLO thermal-hydraulic code in the combined FRAPTRAN-GENFLO code is activated by specifying `genflo='on'` in the `$boundary` block of the FRAPTRAN input file. Besides the general thermal-hydraulic boundary conditions along the test rod, GENFLO also calculates the rod's plenum temperature, and by specifying the input parameter `PlenumTemp=2` (in `$model` block) this value can be used in thermal-mechanical part (FRAPTRAN) of the transient calculations by the FRAPTRAN-GENFLO code. We have used the FEA option for the mechanical analysis of the cladding (`mechan=1` in FRAPTRAN), where for the yield strength the NUREG/CR-6534 correlation in the `ckmn` subroutine of FRAPTRAN is employed. This correlation seems to provide slightly better results in the evaluations of the Halden LOCA tests than the standard yield strength correlation in `ckmn`. The standard FRAPTRAN options `PlenumTemp=0` or `1` cannot be used for this type of test rod and coolant flow. There is also a possibility to specify (prescribe) the plenum temperature as function of time (`PlenumTemp=3`) in VTT's FRAPTRAN version. This option was added to the FRAPTRAN-QT1.4b code for the analyses here.

FRAPTRAN-QT1.4b: In the FRAPTRAN-QT1.4b calculations of the IFA-650 tests, we use the aforementioned FE cladding module combined with certain high-temperature cladding material models introduced in the program (Jernkvist 2010). The extended capability of the code includes models for high-temperature oxidation, phase transformation, creep deformation and rupture. The integrated performance of selected material models for cladding rupture prediction under LOCA conditions has been verified against burst test data in (Manngård and Massih 2010; Manngård and Massih 2011), whereas the performance of individual models is verified and tested in (Massih 2009; Massih 2008). In FRAPTRAN-QT1.4b besides the aforementioned strain-base cladding failure criterion there are stress-base failure criteria after the experimental works of (Erbacher, Neitzel, Rosinger, Schmidt, and Wiehr 1982) and (Rosinger 1984). We have applied Rosinger's average (best-estimate) stress-base failure criterion in our calculations.

The plenum temperature for FRAPTRAN-QT1.4b calculations was either based on thermal-hydraulic calculations (GENFLO) or derived from measured quantities. The plenum temperature variation with time was prescribed using the option `PlenumTemp=3` (cf. also FRAPTRAN-GENFLO paragraph above).

The input options defining the cladding models applied in the FRAPTRAN calculations are summarized in table A1. The cladding model options are set in the `$model` block of the FRAPTRAN input files.



2014:18

The Swedish Radiation Safety Authority has a comprehensive responsibility to ensure that society is safe from the effects of radiation. The Authority works to achieve radiation safety in a number of areas: nuclear power, medical care as well as commercial products and services. The Authority also works to achieve protection from natural radiation and to increase the level of radiation safety internationally.

The Swedish Radiation Safety Authority works proactively and preventively to protect people and the environment from the harmful effects of radiation, now and in the future. The Authority issues regulations and supervises compliance, while also supporting research, providing training and information, and issuing advice. Often, activities involving radiation require licences issued by the Authority. The Swedish Radiation Safety Authority maintains emergency preparedness around the clock with the aim of limiting the aftermath of radiation accidents and the unintentional spreading of radioactive substances. The Authority participates in international co-operation in order to promote radiation safety and finances projects aiming to raise the level of radiation safety in certain Eastern European countries.

The Authority reports to the Ministry of the Environment and has around 300 employees with competencies in the fields of engineering, natural and behavioural sciences, law, economics and communications. We have received quality, environmental and working environment certification.

Strålsäkerhetsmyndigheten
Swedish Radiation Safety Authority

SE-171 16 Stockholm
Solna strandväg 96

Tel: +46 8 799 40 00
Fax: +46 8 799 40 10

E-mail: registrator@ssm.se
Web: stralsakerhetsmyndigheten.se